Adaptation, ancestral variation and gene flow in a 'Sky Island' *Drosophila* species

Tom Hill[1]*, Robert L. Unckless[1]

1. 4055 Haworth Hall, The Department of Molecular Biosciences, University of Kansas, 1200 Sunnyside Avenue, Lawrence, KS 66045.

* Corresponding author: Email: tom.hill@ku.edu

Keywords: *Drosophila innubila,* local adaptation, phylogeography, inversions

Abstract

Over time, populations of species can expand, contract, fragment and become isolated, creating subpopulations that must adapt to local conditions. Understanding how species maintain variation after divergence as well as adapt to these changes in the face of gene flow, is of great interest, especially as the current climate crisis has caused range shifts and frequent migrations for many species. Here, we characterize how a mycophageous fly species, *Drosophila innubila,* came to inhabit and adapt to its current range which includes mountain forests in southwestern USA separated by large expanses of desert. Using population genomic data from more than 300 wild-caught individuals, we examine four populations to determine their population history in these mountain forests, looking for signatures of local adaptation. We find *D. innubila* spread northwards during the previous glaciation period (30-100 KYA), and has recently expanded even further (0.2-2 KYA). *D. innubila* shows little evidence of population structure, consistent with a recent establishment and genetic variation maintained since before geographic stratification. We also find some signatures of recent selective sweeps in chorion proteins and population differentiation in antifungal immune genes suggesting differences in the environments to which flies are adapting. However, we find little support for long-term recurrent selection in these genes. In contrast, we find evidence of long-term recurrent positive selection in immune pathways such as the Toll-signaling system and the Toll-regulated antimicrobial peptides.

Introduction

In the past 25,000 years, the earth has undergone substantial environmental changes due to both human-mediated events (anthropogenic environment destruction, desert expansion, extreme weather and the growing anthropogenic climate crisis) (CLOUDSLEY-THOMPSON 1978; ROSENZWEIG *et al.* 2008) and events unrelated to humans (glaciation and tectonic shifts) (HEWITT 2000; HOLMGREN *et al.* 2003; ARIZONA-GEOLOGICAL-SURVEY 2005). These environmental shifts can fundamentally reorganize habitats, and influence organism fitness, rates of migration between locations, and population ranges (SMITH *et al.* 1995; ASTANEI *et al.* 2005; ROSENZWEIG *et al.* 2008; SEARLE *et al.* 2009; CINI *et al.* 2012; PORRETTA *et al.* 2012; ANTUNES *et al.* 2015). Signatures of the how organisms adapt to these events, or to population migration, are often etched in the patterns of molecular variation within and between species (CHARLESWORTH *et al.* 2003; WRIGHT *et al.* 2003; EXCOFFIER *et al.* 2009).

The Madrean archipelago is an environment currently undergoing extensive environmental change due to the climate crisis, and presents a good model environment to study the genomic consequences of local adaptation and gene flow in a changing environment (SMITH AND FARRELL 2005; COE *et al.* 2012; MANTHEY AND MOYLE 2015; WIENS *et al.* 2019). This range, located in southwestern USA and northwestern Mexico, contains numerous forested mountains known as 'Sky islands', separated by large

expanses of desert (McCormack *et al.* 2009; Coe *et al.* 2012). These 'islands' were connected by woodland forests during the previous glacial maximum which then retreated, leaving montane forest habitat separated by hundreds of miles of desert, presumably limiting migration between locations for most species (Arizona-Geological-Survey 2005; Smith and Farrell 2005; McCormack *et al.* 2009). The islands are hotbeds of ecological diversity. However, due to the changing climate in the past 100 years, they have become more arid and prone to wild fires, which may drive migration, adaptation and even extinction events (McCormack *et al.* 2009; Coe *et al.* 2012; Fave *et al.* 2015; Manthey and Moyle 2015).

Several studies of genetic diversity in Sky Island populations have explored the how species persist in these environments and the extent that gene flow occurs between locations. These studies primarily find that while birds are mostly unstructured (McCormack *et al.* 2009; Manthey and Moyle 2015), flightless species are highly structured (Smith and Farrell 2005; McCormack *et al.* 2009; Fave *et al.* 2015; Wiens *et al.* 2019), due to the difficulty in migrating between these mountains separated by hundreds of miles of desert. These studies also highlight that many species are adapting to the increasingly hot and arid conditions of the Sky Islands, caused by climate change (McCormack *et al.* 2009; Coe *et al.* 2012; Misztal *et al.* 2013). Specifically, several animal species are changing their population distributions in the Sky Islands and adapting to increasingly hostile conditions (Fave *et al.* 2015; Wiens *et al.* 2019). Additionally, the delay in the monsoon period has resulted in several plant species pushing back their flowering period, until adequate water is available (McCormack *et al.* 2009; Crimmins *et al.* 2011).

To date, no studies have considered demographics and local adaptation in the Sky Islands from a whole genome perspective and few have considered demography and local adaptation in insects (Fave *et al.* 2015). Luckily, the Madrean archipelago is inhabited by the ecological *Drosophila* model species, *Drosophila innubila* (Jaenike et al. 2003; Dyer and Jaenike 2005). *Drosophila innubila* is a mycophageous species found throughout these Sky islands and thought to have arrived during the last glacial maximum (Dyer and Jaenike 2005; Dyer *et al.* 2005). This 'island' endemic mushroom-feeder emerges during the rainy season in the Sky Islands for 10-12 weeks in late summer and early fall, before returning to diapause for the winter and dry seasons (Patterson 1954). *D. innubila* and other mycophageous *Drosophila* are well-studied ecologically, giving us a thorough understanding of their life history, environment and pathogens (Shoemaker *et al.* 1999; Perlman *et al.* 2003; Dyer and Jaenike 2005; Dyer *et al.* 2005; Jaenike and Dyer 2008; Unckless 2011; Unckless and Jaenike 2011). For example, *D. innubila* is infected with a male-killing, maternally transmitted pathogen, called *Wolbachia* which has been extensively studied (Jaenike *et al.* 2003; Dyer 2004; Dyer and Jaenike 2005; Dyer *et al.* 2005). *D. innubila* is also frequently exposed to a highly virulent DNA virus (Unckless 2011), as well as toxic mushrooms (Scott Chialvo and Werner 2018). Given these environmental and pathogenic

factors, we expect to identify recent signatures of evolution in the *D. innubila* genome on establishment in the Sky Islands, as well as signatures of a recent population migration.

Newly established populations are almost always small because they usually consist of a few founders (CHARLESWORTH *et al.* 2003; EXCOFFIER *et al.* 2009; LI AND DURBIN 2011). This results in a loss of rare alleles in the population (TAJIMA 1989; GILLESPIE 2004). The population will then grow to fill the carrying capacity of the new niche and adapt to the unique challenges in the new environment, both signaled by an excess of rare alleles (EXCOFFIER *et al.* 2009; WHITE *et al.* 2013). This adaptation can involve selective sweeps from new mutations or standing genetic variation, and signatures of adaptive evolution and local adaptation in genes key to the success of the population in this new location (CHARLESWORTH *et al.* 2003; HERMISSON AND PENNINGS 2005; MCVEAN 2007; MESSER AND PETROV 2013). However, these signals can confound each other making inference of population history difficult. For example, both population expansions and adaptation lead to an excess of rare alleles, meaning more thorough analysis is required to identify the true cause of the signal (WRIGHT *et al.* 2003). Additionally, continual migration between populations can alter the allele frequencies within populations, possibly removing adaptive alleles, or supplying beneficial alleles from other subpopulations (TIGANO AND FRIESEN 2016). Signatures of demographic change are frequently detected in species that have recently undergone range expansion due to human introduction (ASTANEI *et al.* 2005; EXCOFFIER *et al.* 2009) or the changing climate (HEWITT 2000; PARMESAN AND YOHE 2003; GUINDON *et al.* 2010; WALSH *et al.* 2011; CINI *et al.* 2012). Other hallmarks of a range expansion include signatures of bottlenecks visible in the site frequency spectrum, and differentiation between populations (CHARLESWORTH *et al.* 2003; LI AND DURBIN 2011). This can be detected by a deficit of rare variants, a decrease in population pairwise diversity and an increase in the statistic, Tajima's D (TAJIMA 1989). Following the establishment and expansion of a population, there is an excess of rare variants and local adaptation results in divergence between the invading population and the original population. These signatures are also frequently utilized in human populations to identify traits which have fixed upon the establishment of human populations in a new location, or to identify how our human ancestors spread globally (LI AND DURBIN 2011).

Populations with limited migration provide a rare opportunity to observe replicate bouts of evolutionary change and this is particularly interesting regarding coevolution with pathogens, as could be examined in *D. innubila* (DYER AND JAENIKE 2005; UNCKLESS 2011).We sought to reconstruct the demographic and migratory history of *D. innubila* inhabiting the Sky islands to understand if migration is occurring between Sky Islands, and how the species is adapting to its new environment, based on signatures of selection in the genome (TIGANO AND FRIESEN 2016). Additionally, we hoped to determine if populations are locally adapting to their recent environment or if signatures of local adaptation are swamped out by species-level adaptation occurring before population divergence. We resequenced whole genomes

101 of wild-caught individuals from four populations of *D. innubila* in four different Sky island mountain
102 ranges. This differs from most population genomic studies of *Drosophila*, which rely on lab maintained
103 inbred strains. Interestingly, we find little evidence of population structure by location, with structure
104 limited to the mitochondria and a single autosome. However, we do find some signatures of local
105 adaptation, such as for cuticle development and fungal pathogen resistance. We also find evidence of
106 mitochondrial translocations into the nuclear genome, with strong evidence of local adaptation of these
107 translocations, suggesting potential adaptation to changes in metabolic process of the host between location
108 (JAENIKE AND DYER 2008). Finally, we find signatures of long-term selection of the Toll immune pathway,
109 across all populations.

110 **Results**

111 *Drosophila innubila has recently expanded its geographic range and shows little divergence between*
112 *geographically isolated populations*

113 To characterize how *D. innubila* came to inhabit its current range, we collected flies from four Sky island
114 locations across Arizona in September 2017: Chiricahuas (CH, 81 flies), Huachucas (HU, 48 flies), Prescott
115 (PR, 84 flies) and Santa Ritas (SR, 67 flies) (Locations shown in Figure 1). Interestingly, while previous
116 surveys mostly failed to collect *D. innubila* north of the Madrean archipelago in Prescott (DYER AND
117 JAENIKE 2005), we easily sampled from that location, suggesting a possible recent colonization (though we
118 were also unable to collect *D. innubila* in the exact locations previously sampled) (DYER AND JAENIKE
119 2005). If this was a recent colonization event, it could be associated with the changing climate of the area
120 leading to conditions more accommodating to *D. innubila*.

121 To determine when *D. innubila* established in each location and rates of migration between
122 locations, we isolated and sequenced the DNA from our sampled *D. innubila* populations and characterized
123 genomic variation. We then examined the population structure and changes in demographic history of *D.*
124 *innubila* using silent polymorphism in StairwayPlot (LIU AND FU 2015). We found all sampled populations
125 have a current estimated effective population size (N_e) of ~1 million individuals and an ancestral N_e of ~4
126 million individuals, and all experience a bottleneck between 70 and 100 thousand years ago to an N_e of 10-
127 20 thousand (Figure 1, Supplementary Figure 1A & B). This bottleneck coincides with a known glaciation
128 period occurring in Arizona (ARIZONA-GEOLOGICAL-SURVEY 2005). Each surveyed population then
129 appears to go through a population expansion between one and thirty thousand years ago, with populations
130 settling from south to north (Figure 1A, Supplementary Figure 1A & B). Specifically, while the Huachucas
131 population appears to have been colonized first (10-30 thousand years ago), the Prescott population was
132 colonized much more recently (200-2000 years ago). This, and the absence of *D. innubila* in Prescott
133 sampling until ~2016 sampling suggests very recent northern expansion of *D. innubila* (Figure 1). Note,

134 however, that StairwayPlot (LIU AND FU 2015) has estimated large error windows for Prescott, meaning
135 the colonization could be more recent or ancient than the 200-2000 year estimate.
136 The *Drosophila* genome is organized into Muller elements, these are 6 chromosome arms which
137 are generally conserved across all *Drosophila* species, named A to F (with A representing the ancestral
138 *Drosophila* X chromosome) (PATTERSON AND STONE 1949; MARKOW AND O'GRADY 2006; VICOSO AND
139 BACHTROG 2015). While the fusions of these elements differ between *Drosophila* species, the broad
140 synteny is conserved. In our analysis we refer to the chromosomes by their Muller element names, instead
141 of any species-specific chromosome name. Given the geographic distance between populations, we
142 expected to find a corresponding signature of population differentiation across the populations for each
143 Muller element. Using Structure (FALUSH *et al.* 2003), we find surprisingly little population differentiation
144 between locations for each Muller element (Supplementary Figure 1C) but some structure by location for
145 the mitochondrial genome (Supplementary Figure 1D), consistent with previous findings (DYER 2004;
146 DYER AND JAENIKE 2005). Together these suggest that there is either still a large amount of standing
147 ancestral variation shared between populations, or that there is gene flow between populations mostly via
148 males.

149 **Figure 1: A.** Schematic of the route of colonization of *D. innubila*, inferred from population size history
150 based on StairwayPlot results across the four sample locations in Arizona (AZ), Chiracahua's (CH, red),
151 Huachucas (HU, blue), Prescott (PR, green) and Santa Ritas (SR, purple). Stairway plot results used to
152 infer this history are shown in Supplementary Figure 1. **B.** Median pairwise F_{ST} between populations,
153 comparing the autosomal nuclear genome (below diagonal) and the mitochondrial genome (above
154 diagonal).

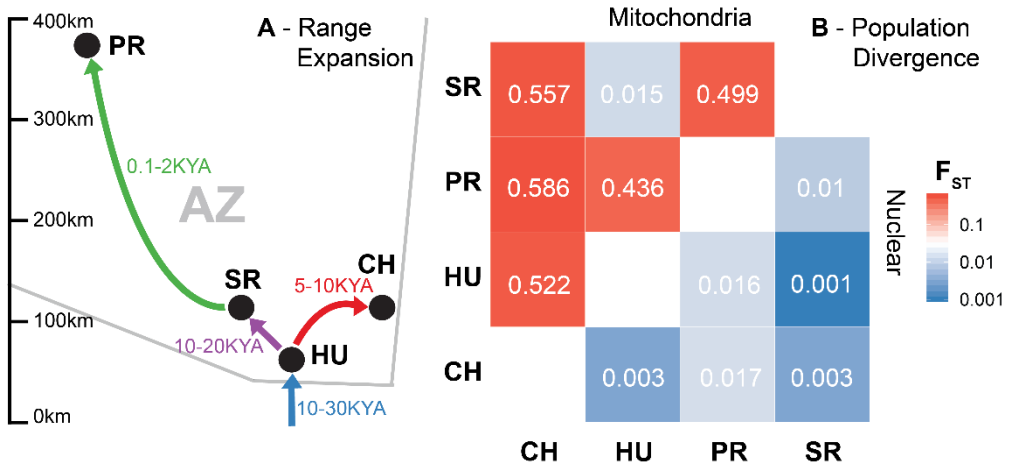

155

156 Given that our populations are either recently established or have high levels of migration, we
157 sought to determine which demographic model best explains the pattern of shared nuclear and

158 mitochondrial variation seen in *D. innubila*. The relatively recent establishment of these populations
159 suggests they may not be at migration-drift balance meaning that F_{ST} may not be an appropriate statistic to
160 determine the extent of gene flow (GUTENKUNST *et al.* 2010; PUZEY *et al.* 2017). Using the silent nuclear
161 polymorphism of each population in δaδi (GUTENKUNST *et al.* 2010), we found the best fitting model for
162 the nuclear variation in each pair of populations. In nearly all cases, the best model was one considering all
163 populations as a single population following a population bottleneck and expansion, as opposed to separate
164 populations with or without migration. This was true whether we considered all variation together or
165 separately for each Muller element (Supplementary Table 3, *p*-value > 0.94). This suggests that the shared
166 variation between populations is due to ancestrally maintained variation as opposed to elevated gene flow
167 homogenizing new mutations arising in particular populations. Contrasting this, we find that the variation
168 in mitochondrial genome fits a model of separate populations with some migration (mean migration rate =
169 0.0525, *p*-value < 0.00794) for all but one pair of populations (HU and SR best fit the model of a single
170 population following a bottleneck, *p*-value = 0.423). This suggests that these populations are recently
171 diverged, and HU and SR should be considered as a single population in all regards (Figure 1). The smaller
172 effective population size of the mitochondrial genome may have resulted in it reaching migration-drift
173 equilibrium faster than the nuclear genome.

174 Though not an appropriate model to determine population divergence, we used F_{ST} as a measure of
175 shared variation (WEIR AND COCKERHAM 1984), and consistent with the δaδi models we find little
176 differentiation between nuclear genomes (Figure 1B). We only find 65,899 nuclear SNPs (~2% of called
177 nuclear SNPs) are exclusive to populations, while most SNPs are shared between at least two populations
178 (Supplementary Figure 2), suggesting most variation is maintained from before each population established
179 separately. In contrast, there is higher F_{ST} between mitochondrial genomes in pairwise comparisons (Figure
180 1B). Both nuclear and mitochondrial δaδi and F_{ST} results are consistent with the Structure/StairwayPlot
181 results (Supplementary Figure 1).

182 We next determined whether the δaδi results were consistent with our expectations about a more
183 recent expansion of *D. innubila* into Prescott. We find the time between population split for Prescott is
184 significantly lower than all other comparisons (GLM t-value = -2.613, *p*-value = 0.0137), and the time since
185 population expansion is also significantly lower for PR than other populations (GLM t-value = -2.313, *p*-
186 value = 0.0275). F_{ST} of the nuclear genome is also significantly higher in Prescott comparisons (Figure 2A,
187 GLM t-value = 93.728, *p*-value = 2.73e-102), though is still extremely low genome-wide in all pairwise
188 comparisons involving PR (PR median = 0.0105), with some outliers on Muller element B like other
189 populations (Supplementary Figures 3 & 4). We also calculated the population genetic statistics pairwise
190 diversity and Tajima's D for each gene using total polymorphism (TAJIMA 1989). As expected with a recent
191 population contraction in Prescott (suggesting recent migration and establishment in a new location),

192 pairwise diversity is significantly lower (Figure 2B, GLM t-value = -19.728, *p*-value = 2.33e-86,
193 Supplementary Table 2) and Tajima's D is significantly higher than all other populations (Figure 2C, GLM
194 t-value = 4.39, *p*-value = 1.15e-05, Supplementary Table 2). This suggests that there is also a deficit of
195 polymorphism in general in Prescott, consistent with a more recent population bottleneck, removing rare
196 alleles from the population (Figure 2C, Supplementary Figure 5). Conversely, the other populations show
197 a genome wide negative Tajima's D, consistent with a recent demographic expansion (Supplementary
198 Figure 5), suggesting a more recent bottleneck in Prescott relative to other populations.

199 **Figure 2: Summary statistics for each population. A.** Distribution of F_{ST} per gene for each population
200 versus all other populations. **B.** Distribution of genic pairwise diversity for each population. **C.** Distribution
201 of genic Tajima's D for each population. **D.** F_{ST} distribution for Antifungal associated genes for each
202 population. **E.** F_{ST} distribution for cuticular proteins for each population. **F.** F_{ST} distribution for all immune
203 genes (excluding antifungal genes). In A, B & C all cases significant differences from CH are marked with
204 an * and outliers are removed for ease of visualization. In D, E & F, significant differences from the genome
205 background in each population are marked with a + and white diamond mark the whole genome average of
206 F_{ST} for each population.

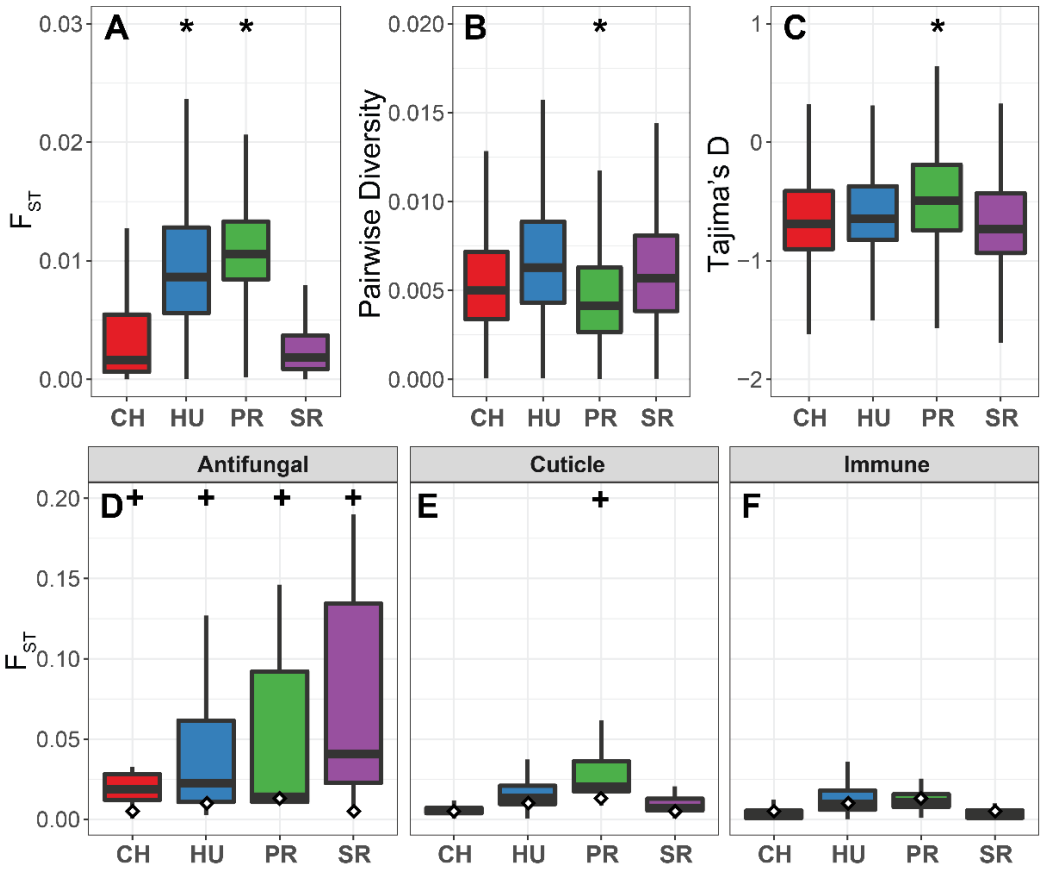

207

208 *Population structure in the D. innubila genome is associated with segregating inversions*
209 Though populations are panmictic for Muller element B (Using δaδi, Supplementary Table 3), F_{ST} is
210 significantly higher on Muller element B compared to all other elements in all populations (Supplementary
211 Figure 3, GLM t-value = 30.02, *p*-value = 3.567e-56) and is enriched for windows in the upper 97.5th
212 percentile of F_{ST} (Supplementary Figure 3, χ^2 test: χ^2 = 79.66, d.f. = 1, *p*-value = 1.06e-16). Additionally,
213 we identified 10kbp windows across the genome in the upper 97.5th percentile for the proportion of
214 population-exclusive SNPs and found Muller B is significantly enriched for population-exclusive SNPs in
215 every population (Supplementary Figure 3 & 4, χ^2 test: χ^2 = 60.28, d.f. = 1, *p*-value = 1.059e-12). All other
216 chromosomes are significantly depleted for population-exclusive SNPs (χ^2 test: χ^2 = 31.90, d.f. = 1, *p*-value
217 = 1.33e-6). On Muller element B, regions of elevated F_{ST} are consistent in all pairwise comparisons between
218 populations (Supplementary Figure 4). Muller element B also has elevated Tajima's D compared to all
219 other Muller elements (Supplementary Figure 5, GLM t-value = 10.402, *p*-value = 2.579e-25), suggesting
220 some form of structured population unique to Muller element B. However, actual values of F_{ST} are still low
221 on Muller element B and populations are considered panmictic when fitting models with δaδi for all 1Mbp
222 windows across Muller element B (Supplementary Table 3) (GUTENKUNST *et al.* 2010), suggesting
223 population structure by location is still minimal (Supplementary Figure 3, Supplementary Table 3, PR
224 Muller B mean = 0.081, Muller C mean = 0.0087, Mitochondrial mean = 0.507).
225 We attempted to identify if this elevated structure is due to chromosomal inversions on Muller
226 element B, comparing F_{ST} of a region to the presence or absence of inversions across windows (using only
227 inversions called by both Delly and Pindel (YE *et al.* 2009; RAUSCH *et al.* 2012)). We find several putative
228 inversions across the genome at appreciable frequencies (89 total above 1% frequency), of which, 37 are
229 found spread evenly across Muller element B and 22 are found at the telomeric end of Muller element A
230 (Figure 3A). The presence of an inversion over a region of Muller element B is associated with higher genic
231 F_{ST} in these regions (Figure 3A, Wilcoxon Rank Sum test W = 740510, *p*-value = 0.0129), though, when
232 calculating F_{ST} for inversions, we find these inversions are not unique or even at different frequencies in
233 specific populations (Mean inversion F_{ST} = 0.024, Max inversion F_{ST} = 0.22, χ^2 test for enrichment in a
234 specific population *p*-value > 0.361 for all inversions). Genes within 10kbp of an inversion breakpoint have
235 significantly higher F_{ST} than outside the inverted regions, consistent with findings in other species (Figure
236 3C, GLM t-value = 7.702, *p*-value = 1.36e-14) (MACHADO *et al.* 2007; NOOR *et al.* 2007). However, genes
237 inside inverted regions show no difference in F_{ST} compared to those outside (Figure 3C, GLM t-value = -
238 0.178, *p*-value = 0.859). All regions of Muller element B have higher F_{ST} than the other Muller elements
239 (Figure 3C, outside inversions Muller element B vs all other chromosomes: GLM t-value = 7.379, *p*-value
240 = 1.614e-13), suggesting some chromosome-wide force drives the higher F_{ST} and Tajima's D, opposed to
241 reduced recombination near inversion breakpoints (NOOR *et al.* 2007).

Given that calls for large inversions in short read data are often not well supported (CHAKRABORTY *et al.* 2017) and the apparently complex nature of the Muller element B inversions (Figure 3A), we may not have correctly identified the actual inversions and breakpoints on the chromosome. Despite this, our results do suggest a link between the presence of inversions on Muller element B and elevated differentiation of the entire Muller element B between *D. innubila* populations.

Figure 3: Summary of the inversions detected in the *Drosophila innubila* populations. **A.** Location and frequency in the total population of segregating inversions at higher than 1% frequency and greater than 100kbp. Shaded bars highlight the beginning and end of each inversion (X-axis) on each chromosome, as well as the inversion frequency (Y-axis). **B.** Tajima's D and **C.** F_{ST} for genes across Muller element B, grouped by their presence under an inversion, outside of an inversion, near the inversion breakpoints (within 10kbp) or on a different Muller element. All inversions and frequencies inferred compared to the reference *D. innubila* genome.

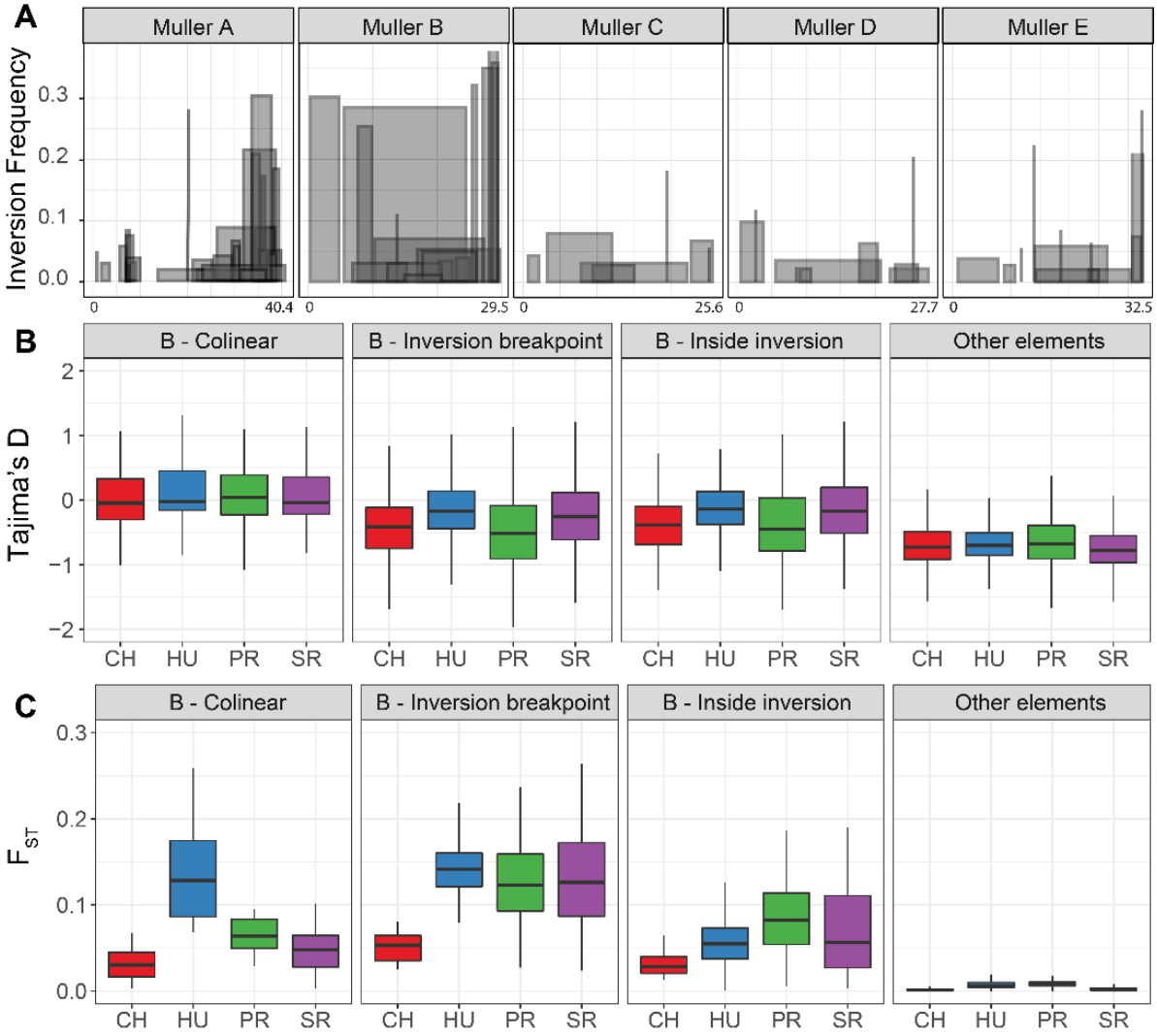

255 *Evidence for increased population differentiation in antifungal and cuticle development genes*
256 Though differentiation is low across most of the genome in each population as populations are recently
257 established and most variants are shared, we still find several genomic regions with relatively elevated
258 differentiation, using F_{ST} as a proxy for divergence. In addition to the entirety of Muller element B, there
259 are narrow windows of high F_{ST} on Muller elements D and E (Figure 4, Supplementary Figure 3 & 4). We
260 attempted to identify whether any gene ontology groups have significantly higher F_{ST} than the rest of the
261 genome. We consider a peak of elevated F_{ST} to be genes in the upper 97.5th percentile of F_{ST} on each
262 chromosome. These peaks for F_{ST} are enriched for antifungal genes in all populations and all in pairwise
263 comparisons (Figure 2D, Supplementary Table 4, GO enrichment = 16.414, *p*-value = 1.61e-10). These
264 antifungal genes (including *Dif, cactus* and *Trx-2* in all populations, *grass* in PR, and *modSP* in CH) are
265 distributed across the genome and so not all under one peak of elevated $F_{ST.}$ Interestingly, this is the only
266 immune category with elevated F_{ST} (Figure 2F), with most of the immune system showing no signatures of
267 increased divergence between populations (Figure 2F, Supplementary Figure 6). This suggests that that
268 fungal pathogens apply the strongest divergent selective pressure among populations.
269 Genes related to cuticle development also have significantly higher F_{ST}, when compared to all other
270 genes (Figure 2E, Supplementary Table 4, GO enrichment = 5.03, *p*-value = 8.68e-08), which could be
271 associated with differences in the environment between locations (toxin exposure, humidity, *etc*.).
272 Consistent with this result, the peak of F_{ST} on Muller element D (Figure 5, Muller element D, 11.56-
273 11.58Mb) is composed exclusively of genes involved in cuticle development (e.g. *Cpr65Au*, *Cpr65Av*,
274 *Lcp65Ad*) with elevated F_{ST} in these genes in all pairwise comparisons involved SR and HU, and the one
275 vs all SR and HU population comparisons as well as PR comparisons (Figure 5), suggesting that they may
276 be adapting to differing local conditions in those populations.
277 Two other clear peaks of elevated F_{ST} on Muller element E are also composed of genes in similar
278 genomic categories (e.g. cuticle development). There also appears to be three regions of the *D. innubila*
279 genome with translocated mitochondrial genes (Figure 5). The first peak (Muller element E, 11.35-11.4Mb)
280 is composed exclusively of one of these translocated mitochondrial regions with 3 mitochondrial genes
281 (including *cytochrome oxidase II*). The second peak (Muller element E, 23.60-23.62Mb) contains four other
282 mitochondrial genes (including *cytochrome oxidase III* and *ND5*) as well as genes associated with nervous
283 system activity (such as *Obp93a* and *Obp99c*). We find no correlation between coverage of these regions
284 and mitochondrial copy number (Supplementary Table 1, Pearsons' correlation t-value = 0.065, *p*-value =
285 0.861), so this elevated F_{ST} is probably not an artefact of mis-mapping reads. However, we do find these
286 regions have elevated copy number compared to the rest of the genome (Supplementary Figure 7, GLM t-
287 value = 9.245, *p*-value = 3.081e-20), and so this elevated divergence may be due to collapsed paralogs.
288 These insertions of mtDNA are also found in *D. falleni* and are diverged from the mitochondrial genome,

289 suggesting ancient transpositions (HILL *et al.* 2019). The nuclear insertions of mitochondrial genes are also
290 enriched in the upper 97.5th percentile for F_{ST} in HU and PR, when looking at only autosomal genes
291 (Supplementary Table 4, GO enrichment = 4.53, *p*-value = 3.67e-04). Additionally, several other energy
292 metabolism categories are in the upper 97.5th percentile for F_{ST} for all pairwise comparisons involving CH.
293 We find peaks of elevated pairwise diversity exclusively on the mitochondrial translocations
294 (Supplementary Figure 8), suggesting unaccounted for variation in these genes which is consistent with
295 duplications detected in these genes (RASTOGI AND LIBERLES 2005) (Supplementary Figure 7). This
296 supports the possibility that unaccounted for duplications may be causing the elevated F_{ST} pairwise diversity
297 in mitochondrial genes (Supplementary Figures 6-8). Overall these results suggest a potential divergence
298 in the metabolic needs of each population, and that several mitochondrial genes may have found a new
299 function in the *D. innubila* genome and may be diverging (and changing in copy number, Supplementary
300 Figure 7) due to differences in local conditions.

301 **Figure 4:** Comparison of estimated statistics across the *D. innubila* genome for the Prescott (PR)
302 population. Values are as follows: the average pairwise divergence per gene (D_{XY}, Prescott vs. all other
303 populations), the gene wise population fixation index (F_{ST}, Prescott vs. all other populations), within
304 population pairwise diversity per genes, Composite Likelihood Ratio (CLR) per SNP calculated using
305 Sweepfinder2, and gene wise within population Tajima's D. For D_{XY}, F_{ST}, Pairwise Diversity and Tajima's
306 D, Genes or windows in the upper 97.5th percentile per chromosome are colored red. The lower 2.5th
307 percentile per chromosome is also colored in red for Tajima's D. For Composite Likelihood Ratio the upper
308 99th percentile windows are colored red. Shaded regions on the F_{ST} plot are further examined in Figure 5.

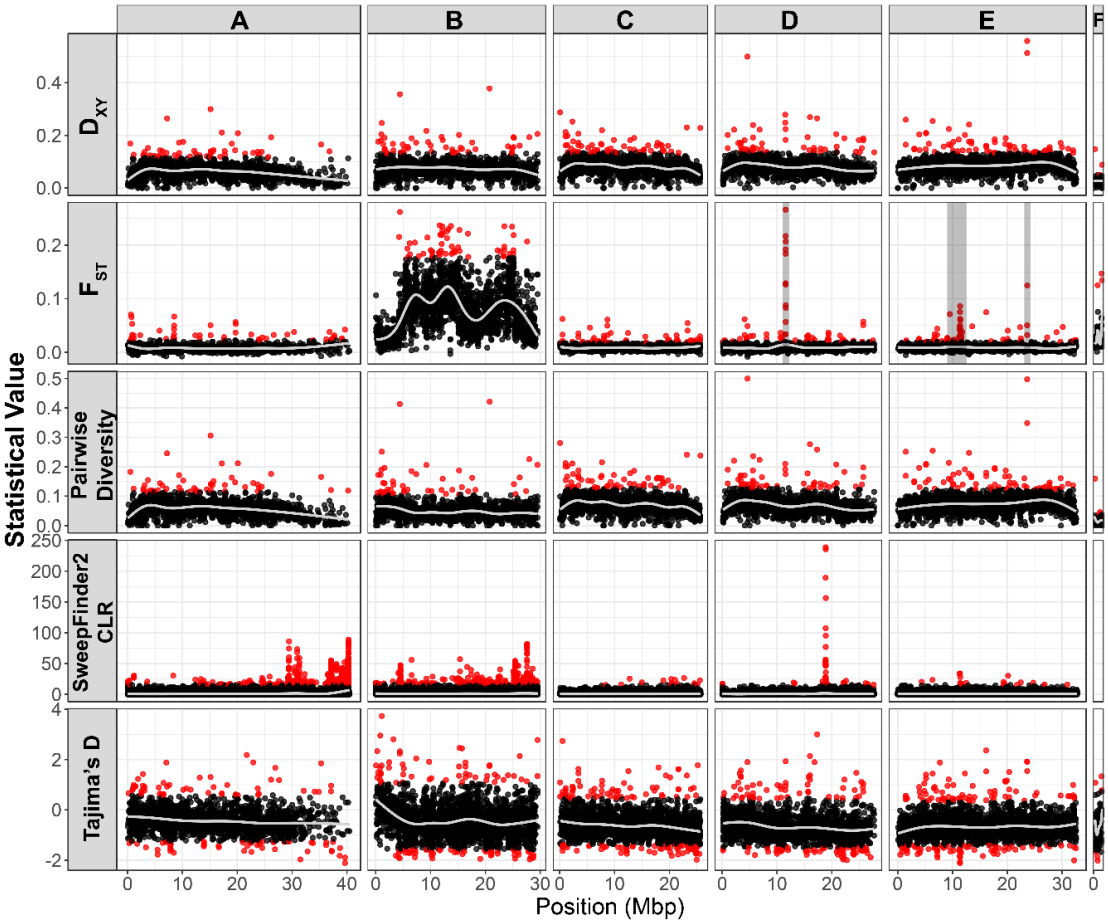

There has been considerable discussion over the last several years about the influence of demographic processes and background selection on inference of local adaptation (CUTTER AND PAYSEUR 2013; CRUICKSHANK AND HAHN 2014; HOBAN *et al.* 2016; MATTHEY-DORET AND WHITLOCK 2018). In contrast to F_{ST} which is a relative measure of population differentiation, D_{XY} is an absolute measure that may be less sensitive to other population-level processes (NEI 1987; CRUICKSHANK AND HAHN 2014). In our data, the upper 97.5th percentile for F_{ST} also significantly overlaps with the upper 97.5th percentile for D_{XY} (Figure 4, Supplementary Figures 3, 4 & 8, χ^2 text: $\chi^2 = 62.61$, p-value = 2.54e-14). The upper 97.5th percentile for D_{XY} is enriched for chorion proteins in all pairwise comparisons and antifungal proteins for all pairwise comparisons involving PR (Supplementary Table 6, p-value < 0.05). Further, the high peak of F_{ST} over Muller element D cuticle proteins seen in all populations is also present when using D_{XY} (Figure 4). We find no evidence for duplications in the antifungal, cuticle or chorion proteins, suggesting the elevated F_{ST} and D_{XY} is likely due to local adaptation and not because of unaccounted for copy number variation (Figure 4, Supplementary Figure 7).

Figure 5: Gene-wise F_{ST} showing regions of elevated divergence between populations for each population. Plot shows F_{ST} for each gene in these regions to identify the causal genes. Genes with noted functions (cuticle development or mitochondrial translocations) are shown by point shape. Note the Y-axes are on different scales for each plot. Genes in the upper 97.5th percentile of F_{ST} on each chromosome are colored in red.

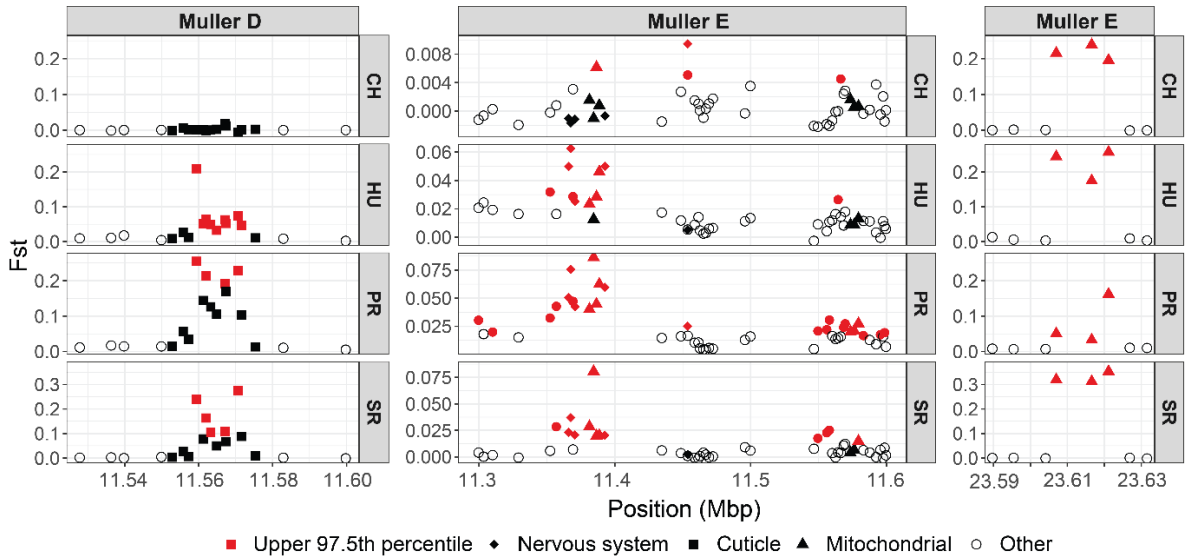

Evidence for recent selective sweeps in chorion genes in each population

Recent adaptation often leaves a signature of a selective sweep with reduced polymorphism near the site of the selected variant. We attempted to identify selective sweeps in each population (and identify similar selective sweeps in multiple populations) using Sweepfinder2 to calculate the composite likelihood of a selective sweep (HUBER *et al.* 2016). We first assessed if percentile of F_{ST} and composite likelihood overlap, suggesting that the elevated F_{ST} is due to a recent selective sweep (NIELSEN 2005). We find no evidence of selective sweeps overlapping with genes with elevated F_{ST} (Supplementary Figure 9A, χ^2 test for overlap of 97.5th percentile windows $\chi^2 = 1.33$ p-value = 0.249), suggesting that the divergence between populations is likely not because of local adaptation. This is consistent with the high levels of ancestrally maintained variation we find and the recent establishment of each population (Figure 1). The upper 97.5th percentile of composite likelihood is equally distributed across the genome and are not enriched for any gene ontology categories (p-value > 0.31), but if we limit our survey, we find the upper 99th percentile is enriched for chorion/egg development genes in all populations (Enrichment = 5.12, p-value = 0.00351).

We find one peak of extremely high composite likelihood values present in all populations on Muller element D, but most extreme in Prescott (Figure 4, Supplementary Figure 9B, Muller D, 18.75-19Mb). The center of this peak is upstream of the cuticle protein *Cpr66D* and four chorion proteins (*Cp15, Cp16, Cp18, Cp19*), with several cell organization proteins (*Zasp66, Pex7, hairy, Prm, Fhos*) within 10kbp

346 of the sweep center. These specific chorion proteins do not have elevated F_{ST} or D_{XY} compared to the rest
347 of the genome (Wilcoxon Rank Sum W = 399170, *p*-value = 0.273), but has significantly elevated D_{XY}
348 compared to other genes within 50kbp (Supplementary Figures 8 & 9, Wilcoxon Rank Sum W = 45637000,
349 *p*-value = 0.0158). However, this may be due to the reduced diversity seen in these chorion genes because
350 of the selective sweep (McVean 2007).

351 Finally, we find evidence of several peaks of selective sweeps in the non-recombining telomere of
352 the X chromosome (Muller A, 39.5-40.5Mb), among several uncharacterized genes (Supplementary Figure
353 9). Consistent with this, we find F_{ST} is elevated between our 2001 and 2017 Chiricahua samples, suggesting
354 at least one recent sweep on the X telomere (Supplementary Figure 10A), resulting in different variants
355 fixing in the 16 years between samplings.

356 *Toll-related immune show signatures of recurrent positive selection in D. innubila*

357 Finally, we sought to if identify genes and functional categories showing strong signatures of selective
358 sweeps and divergence are also undergoing adaptive evolution, suggesting species-wide long-term
359 evolution as opposed to recent adaptation. We reasoned that if the elevated population differentiation seen
360 in antifungal genes and cuticle development proteins (Figure 2 & 3, Supplementary Figure 6) was due to
361 adaptation also acting over longer time periods, we would expect to see signatures of ancient adaptation in
362 those categories. Furthermore, Hill *et al.* used d_N/d_S-based statistics to show that genes involved in some
363 immune defense pathways were among the fastest evolving genes in the *D. innubila* genome (Hill *et al.*
364 2019). We also sought to identify what genes are evolving due to recurrent positive selection in *D. innubila*
365 in one or all populations. To this end we calculated the McDonald-Kreitman based statistic direction of
366 selection (DoS) (Stoletzki and Eyre-Walker, 2011) and SnIPRE selection effect (Eilertson et al., 2012) to
367 estimate the proportion of substitutions fixed by adaptation and identify genes under recurrent selection.
368 We then fit a linear model to identify gene ontology groups with significantly higher DoS or selection effect
369 than expected. In this survey we found cuticle genes and antifungal genes did have some signatures of
370 adaptive evolution (DoS > 0, Selection Effect > 0 and significant McDonald-Krietman test for 80% of genes
371 in these categories) but as a group showed no significant differences from the background (GLM t-value =
372 1.128, *p*-value = 0.259, Supplementary Table 5). In fact, we only found two functional groups significantly
373 higher than the background, Toll signaling proteins (GLM t-value = 2.581 *p*-value = 0.00986,
374 Supplementary Table 4) and antimicrobial/immune peptides (AMPs, GLM t-value = 3.66 *p*-value =
375 0.00025, Supplementary Table 4). In a previous survey we found that these categories also had significantly
376 elevated rates of amino acid divergence (Hill *et al.* 2019). These results suggest that this divergence is
377 indeed adaptive. We find no evidence that genes under recent selective sweeps are undergoing recurrent
378 evolution, suggesting these genes are only recent targets of selection (Supplementary Table 4).

379 Five immune peptides showed consistently positive DoS and selection effect values (which are also
380 among the highest in the genome): four *Bomanins* and *Listericin*. The *Bomanins* are immune peptides
381 regulated by Toll signaling, while JAK-STAT regulates *Listericin* (HOFFMANN 2003; TAKEDA AND AKIRA
382 2005). *Listericin* has been implicated in the response to viral infection due to its expression upon viral
383 infection (DOSTERT *et al.* 2005; ZAMBON *et al.* 2005; IMLER AND ELFTHERIANOS 2009; MERKLING AND
384 VAN RIJ 2013), additionally Toll-regulated AMPS have been shown to interact with the dsDNA Kallithea
385 virus in *Drosophila melanogaster* (PALMER et al. 2018). *D. innubila* is burdened by Drosophila innubila
386 nudivirus (DiNV), a Nudivirus closely related to Kallithea virus, that infects 40-80% of individuals in the
387 wild (UNCKLESS 2011; HILL AND UNCKLESS 2020). Consistent with the adaptation observed in Toll
388 signaling proteins, this suggests the Toll immune system is under long term selection to resist infection by
389 this DNA virus. However, Toll is also the major component of humoral defense against Gram-positive
390 bacteria and fungi (KIMBRELL AND BEUTLER 2001). Since *D. innubila* feed and breed in rotting mushrooms
391 (JAENIKE AND PERLMAN 2002), we can't rule out that the recurrent adaptation in Toll genes is related to
392 adaptation to the conditions of their pathogen-infested habitats. For all immune categories, as well as cuticle
393 proteins and antifungal proteins, we find no significant differences between populations for either MK-
394 based statistics, and no significant differences in the distribution of these statistics between populations
395 (GLM t-value < 0.211, p-value > 0.34 for all populations, Supplementary Table 4). Selection at these loci
396 is likely long term due to an ancient selective pressure and has been occurring since before the separation
397 of these populations. Mutation rates, efficacy of selection and population structure can vary across the
398 genome, which can confound scans for selection (CHARLESWORTH *et al.* 2003; STAJICH AND HAHN
399 2005).To work around this, we employed a control-gene resampling approach to identify the average
400 difference from the background for each immune category (CHAPMAN *et al.* 2019). We find no signatures
401 of ancient positive selection in antifungal genes (Supplementary Figure 11, 61% resamples > 0) or cuticle
402 genes (Figure 6, 54% resamples > 0) but do again find extremely high levels of positive selection in AMPs
403 (Figure 6, 100% resamples > 0) and Toll signaling genes (Figure 6, 99.1% resamples > 0). Segregating
404 slightly deleterious mutations can bias inference of selection using McDonald-Kreitman based tests
405 (MESSER AND PETROV 2012). To further account for this bias, we also calculated asymptotic α for all
406 functional categories across the genome (HALLER AND MESSER 2017). As before, while we find signals for
407 adaptation in antifungal and cuticle proteins (asymptotic α > 0), values in both categories do not differ from
408 the background (Supplementary Figure 11, permutation test Antifungal *p*-value = 0.243, Cuticle *p*-value =
409 0.137). As with the basic McDonald-Kreitman statistics (Figure 6), the only categories significantly higher
410 than the background are Toll signaling genes (Permutation test *p*-value = 0.033) and AMPs (Permutation
411 test *p*-value = 0.035). Together these results suggest that while genes involved in antifungal resistance and
412 cuticle development are slightly divergent between populations (Figure 5), this evolution has likely not

been occurring over long-time scales and so is restricted to their current environments. Alternatively, the adaptation may be too recent to detect a signal using polymorphism and divergence-based metrics. In either case, signals of longer-term adaptation in *D. innubila* appear to be driven by host-pathogen interactions (possibly with the long-term viral infection DiNV (HILL *et al.* 2019)) as opposed to local adaptation.

Figure 6: McDonald-Kreitman based statistics for immune categories in *D. innubila* and cuticle development. The left two plots show estimated statistics (Direction of Selection and Selection Effect) for each gene. The right two plots show the difference in mean statistic (Direction of Selection and Selection Effect) for each gene and a randomly sampled nearby gene.

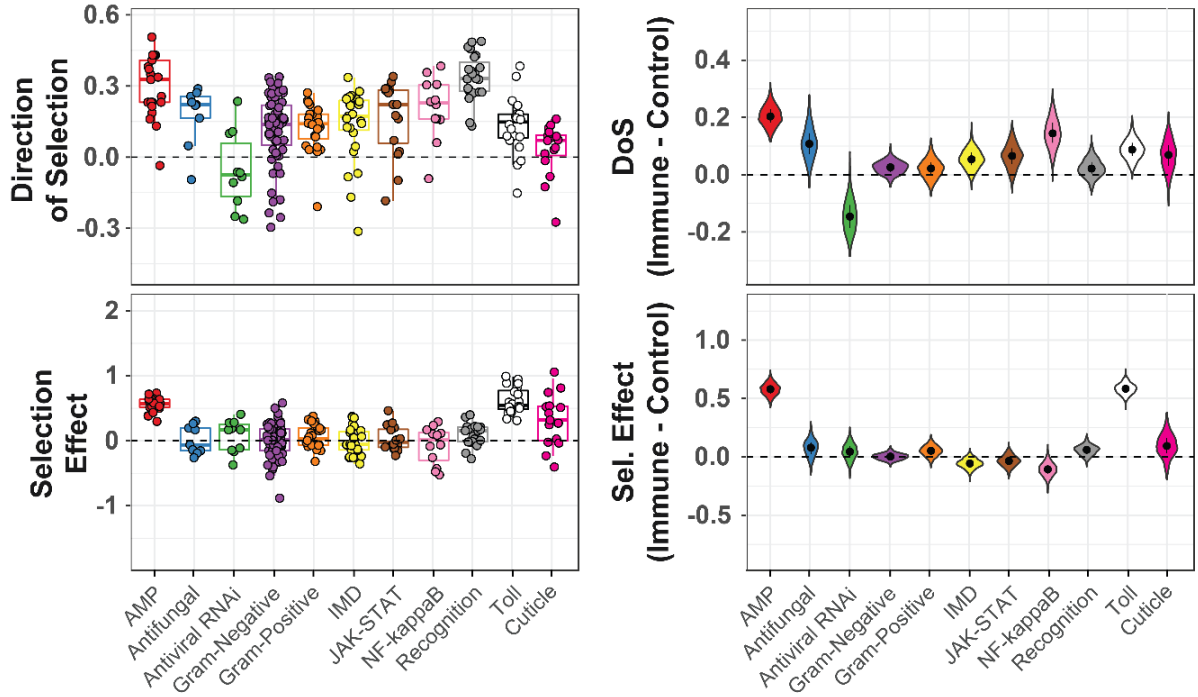

Discussion

Interpopulation divergence is a time-dependent process where pro-divergence factors of genetic drift and local adaptation oppose ancestral variation and migration (RANKIN AND BURCHSTED 1992; GILLESPIE 2004; EXCOFFIER *et al.* 2009; WHITE *et al.* 2013). We sought to examine the extent that these factors drive divergence, and the genomic basis of colonization, divergence and local adaptation in *Drosophila innubila,* a geographically structured species found across four forests separated by large expanses of desert. We characterized the phylogeographic history of four populations of *Drosophila innubila* (Figure 7), a mycophagous species endemic to the Arizonan Sky islands using whole genome resequencing of 318 wild-caught individuals. *D. innubila* expanded into its current range during or following the previous glacial maximum (Figure 1, Supplementary Figure 1). Interestingly, there is very little support for population structure across the nuclear genome (Figures 1 & 2, Supplementary Figures 1-4), including in the repetitive

content (Supplementary Figure 12), but some evidence of population structure in the mitochondria, as found previously in *D. innubila* (DYER AND JAENIKE 2005). There are two models which could explain this pattern: the first is extremely high migration, but of mostly males (as seen in other disparate species (RANKIN AND BURCHSTED 1992; SEARLE *et al.* 2009; MA *et al.* 2013; AVGAR AND FRYXELL 2014)), resulting in a panmictic nuclear genome but diverged mitochondrial genome (as shown in Figure 1B). The second model (which we found better support for using δaδi, Supplementary Table 3) is that ancestral variation is maintained due to the recent isolation of populations (less than $4N_e$ generations ago) and recent coalescent times (Figure 1B, Supplementary Figure 3), though the elevated mutation rate and reduced N_e of the mitochondria results in an increased rate of differentiation by drift between mitochondrial genomes (GILLESPIE 2004). Similarly, Drosophila innubila Nudivirus, a DNA virus infecting *Drosophila innubila,* is also highly structured, possibly due to the smaller N_e, elevated mutation rate and high levels of adaptation (HILL AND UNCKLESS 2020). *D. innubila* is also parasitized by a male-killing strain of the maternally transmitted, intracellular bacterium, *Wolbachia.* This alphaproteobacterium infects about 65% of arthropods (WERREN *et al.* 2008), and has evolved several strategies to improve their chances of transmission between generations, including killing male offspring in *D. innubila* (DYER AND JAENIKE 2005; DYER *et al.* 2005; JAENIKE AND DYER 2008; WERREN *et al.* 2008). The mitochondrial divergence could be driven by linkage to the *Wolbachia*: when *Wolbachia* variants sweep (such as variants that improve parasitism), mitochondrial variants will hitchhike to fixation (JAENIKE *et al.* 2003; DYER AND JAENIKE 2005). This will then further decrease the effective population size of the mitochondria, reaching migration-drift equilibrium faster than expected for a haploid genome under drift.

Figure 7: Summary of signatures of selection (Selective sweeps) and population differentiation (F_{ST} & D_{XY}) shown on the phylogeny of *Drosophila innubila* populations. Signals seen as divergence between all populations (F_{ST}) or recurrent/long-term evolution (McDonald-Kreitman, MK) is shown in black and grey respectively on the left-hand side. Signals seen on each branch are colored by the branches that the signals are seen on, shown on the right-hand side.

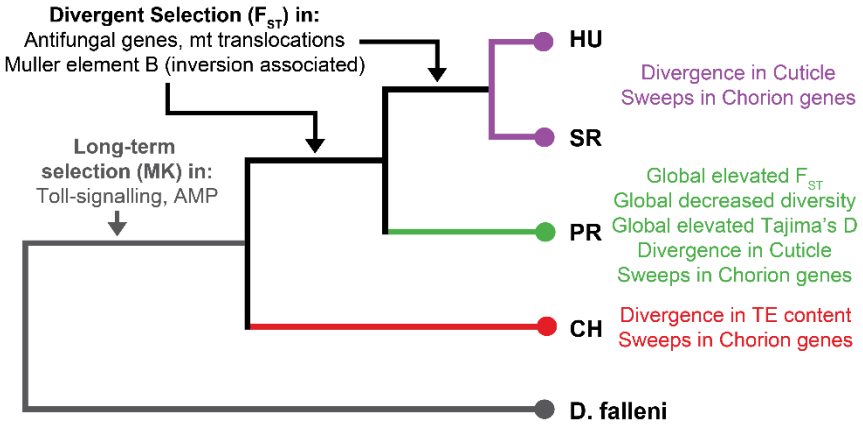

459 Most Sky Island species are highly diverged between locations, suggesting that *D. innubila* may be
460 much more recently established than other species (SMITH AND FARRELL 2005; FAVE *et al.* 2015; WIENS
461 *et al.* 2019). Similar patterns of limited nuclear divergence between species are observed in a Sky Island
462 bird species, *S. carolinensis* (MANTHEY AND MOYLE 2015), however this flying species can easily migrate
463 between Sky Islands (MANTHEY AND MOYLE 2015). In contrast, the patterns observed in *D. innubila*
464 populations are more likely ancestrally maintained and not due to gene flow (Figure 1 & 2, Supplementary
465 Figure 2). In *S. carolinensis,* differential selection is restricted to loci associated with recent changes in
466 environmental extremes (MANTHEY AND MOYLE 2015). This may also be the case in *D. innubila*, as we
467 find some evidence of recent selection, limited to genes associated with environmental factors, chorion
468 genes and antifungal immune genes. (Figure 7, Supplementary Figure 2). Most other insect and non-flying
469 species found across the Sky Islands are highly structured between locations (SMITH AND FARRELL 2005;
470 FAVE *et al.* 2015; WIENS *et al.* 2019). If the lack of geographic divergence is due to the maintenance of
471 ancestral variation, we expect *D. innubila* populations to become as structured as these other species over
472 time.
473 Segregating inversions are often associated with population structure (DOBZHANSKY AND
474 STURTEVANT 1937; FULLER *et al.* 2016; PUZEY *et al.* 2017) and could explain the excess interpopulation
475 divergence seen on Muller element B here (Supplementary Figures 2-5). Our detection of several putative
476 segregating inversions on Muller element B relative to all other chromosomes (Figure 3A) supports this
477 assertion. However, all are large and common inversions characterized in all populations, suggesting the
478 inversions are not driving the elevated F_{ST}. We suspect that the actual causal inversions may not have been
479 correctly characterized for two reasons. First there are limitations of detecting inversions in repetitive
480 regions with short read data (MARZO *et al.* 2008; CHAKRABORTY *et al.* 2017). Second, and confounding
481 the first, the likely existence of several overlapping segregating inversions complicates correctly calling
482 inversion breakpoints further. The elevated F_{ST} could also be caused by other factors, such as extensive
483 duplication and divergence on Muller element B being misanalysed as just divergence. In fact, the broken
484 and split read pairs used to detect inversions are very similar to the signal used to detect duplications (YE
485 *et al.* 2009; RAUSCH *et al.* 2012; CHEN *et al.* 2016), suggesting some misidentification may have occurred.
486 If a large proportion of Muller B was duplicated, we would see elevated mean coverage of Muller element
487 B in all strains compared to other autosomes, which is not the case (Supplementary Table 1). There may
488 also be seasonal variation in inversions which causes the elevated Tajima's D and F_{ST} seen here
489 (Supplementary Figures 3-5) and may be the cause of the difference in minor allele frequency between
490 2001 and 2017 on Muller element B (Supplementary Figure 10B). In fact, in several species, inversions can
491 change in frequency as the multiple linked variants they contain change in fitness over time (RODRIGUEZ-
492 TRELLES *et al.* 1996; ONEAL *et al.* 2014; KAPUN *et al.* 2016; PUZEY *et al.* 2017).

While we find no differences in inversion frequencies between time points (2001 and 2017) in *D. innubila* (Wilcoxon Rank Sum Test W = 561, *p*-value = 0.352), we again may not have correctly identified the inversions and so cannot properly infer frequency changes. Segregating inversions, such as those on Muller element B, are frequently associated with local or temporal variation (DOBZHANSKY AND STURTEVANT 1937; RODRIGUEZ-TRELLES *et al.* 1996; ONEAL *et al.* 2014), and consistent with this find differences in allele frequencies between time points (Supplementary Figure 10B). There was an extensive forest fire in the Sky Islands in 2011 which could plausibly have been a strong selective force driving a change in allele frequency on Muller B between time points (Supplementary Figure 10B) (ARECHEDERRA-ROMERO 2012). It is also worth noting that *D. pseudoobscura* segregates for inversions on Muller element C and these segregate by population in the same Sky island populations (and beyond) as the populations described here (DOBZHANSKY AND STURTEVANT 1937; DOBZHANSKY *et al.* 1963; FULLER *et al.* 2016). The inversion polymorphism among populations is a plausible area for local adaptation and may provide an interesting contrast to the well-studied *D. pseudoobscura* inversions. (HERMISSON AND PENNINGS 2005; MCVEAN 2007; PRZEWORSKI *et al.* 2011).

Ours is one of few studies that sequences whole genomes from individual wild-caught *Drosophila* and therefore avoids several generations of inbreeding that would purge recessive deleterious alleles (GILLESPIE 2004; MACKAY *et al.* 2012; POOL *et al.* 2012). During inbreeding (or due to unintentional inbreeding over generations as lines are maintained) a large proportion of variation found in the population will be removed by background selection (CHARLESWORTH *et al.* 1993). This limits the scope of studies, and the ability to infer the history of the population. Additionally, when attempting to calculate the extent of adaptation occurring in populations, inbred panels will have removed a large proportion of segregating (likely deleterious) variation, which may lead to misestimations of McDonald-Kreitman based statistics, which normalize divergence to polymorphism (MCDONALD AND KREITMAN 1991A; EILERTSON *ET AL.* 2012; MESSER AND PETROV 2012). This could also explain the excessive rates of adaptation in *Drosophila melanogaster* compared to other species (CAI *et al.* 2009; SELLA *et al.* 2009). The excess of putatively deleterious alleles which may be present in our study harkens back to early studies of segregating lethal mutations in populations as well as recent work on humans (DOBZHANSKY *et al.* 1963; MARINKOVIC 1967; DOBZHANSKY AND SPASSKY 1968; WATANABE *et al.* 1974; GAO *et al.* 2015).

To date, most of the genomic work concerning the phylogeographic distribution and dispersal of different *Drosophila* species has been limited to the *melanogaster* supergroup (POOL *et al.* 2012; POOL AND LANGLEY 2013; BEHRMAN *et al.* 2015; LACK *et al.* 2015; MACHADO *et al.* 2015), with some work in other *Sophophora* species (FULLER *et al.* 2016). This limits our understanding of how non-commensal species disperse and behave, and what factors seem to drive population demography over time. Here we have glimpsed into the dispersal and history of a species of mycophageous *Drosophila* and found evidence of

527 changes in population distributions potentially due to the changing climate (Figure 7) (ARIZONA-
528 GEOLOGICAL-SURVEY 2005) and population structure possibly driven by segregating inversions. Because
529 many species have recently undergone range changes or expansions (EXCOFFIER *et al.* 2009; PORRETTA *et*
530 *al.* 2012; WHITE *et al.* 2013), we believe examining how this has affected genomic variation is important
531 for population modelling and even for future conservation efforts (EXCOFFIER *et al.* 2009; COE *et al.* 2012).

532 **Methods**

533 *Fly collection, DNA isolation and sequencing*

534 We collected wild *Drosophila* at the four mountainous locations across Arizona between the 22nd of August
535 and the 11th of September 2017: the Southwest research station in the Chiricahua mountains (CH, ~5,400
536 feet elevation, 31.871 latitude -109.237 longitude, 96 flies), in Prescott National Forest (PR, ~7,900 feet
537 elevation, 34.586 latitude -112.559 longitude, 96 flies), Madera Canyon in the Santa Rita mountains (SR,
538 ~4,900 feet elevation, 31.729 latitude -110.881 longitude, 96 flies) and Miller Peak in the Huachuca
539 mountains (HU, ~5,900 feet elevation, 31.632 latitude -110.340 longitude, 53 flies) (COE *et al.* 2012).
540 *Drosophila innubila* only emerge for a short period of time in the Arizona wet season (~2 months), limiting
541 dates of collection to this period of time each year (PATTERSON AND STONE 1949). Baits consisted of store-
542 bought white button mushrooms (*Agaricus bisporus*) placed in large piles about 30cm in diameter, with at
543 least 5 baits per location. We used a sweep net to collect flies over the baits in either the early morning or
544 late afternoon between one and three days after the bait was set. We sorted flies by sex and species at the
545 University of Arizona in Tucson, AZ and flash frozen at -80°C before shipping on dry ice to the University
546 of Kansas in Lawrence KS.

547 We sorted 343 flies (172 females and 171 males) which phenotypically matched *D. innubila.* We
548 then homogenized and extracted DNA using the Qiagen Gentra Puregene Tissue kit (USA Qiagen Inc.,
549 Germantown, MD, USA), isolating DNA for each fly individually. We also isolated the DNA of 40 *D.*
550 *innubila* samples individually, collected in early September in 2001 from CH. We prepared a genomic DNA
551 library of these 383 DNA samples using a modified version of the Nextera DNA library prep kit (~ 350bp
552 insert size) meant to conserve reagents, during this process we barcoded each sample to distinguish
553 individuals during sequencing. We sequenced the libraries on four lanes of an Illumina HiSeq 4000 (150bp
554 paired end) (Supplementary Table 1, Data deposited in the NCBI SRA: SRP187240).

555 *Sample filtering, mapping and alignment*

556 We removed adapter sequences using Scythe (BUFFALO 2018), trimmed all data using cutadapt to remove
557 barcodes (MARTIN 2011) and removed low quality sequences using Sickle (parameters: -t sanger -q 20 -l
558 50) (JOSHI AND FASS 2011). We masked the *D. innubila* reference genome, using *D. innubila* TE sequences
559 generated previously and RepeatMasker version 4.0 (parameters: -s -gccalc -gff -lib customLibrary) (SMIT

560 AND HUBLEY 2013-2015; HILL *et al.* 2019). We then mapped the short reads to the masked *D. innubila*
561 genome using BWA MEM Version 0.7.17 (LI AND DURBIN 2009), and sorted and indexed using SAMTools
562 Version 1.9 (LI *et al.* 2009). Following mapping, we added read groups, marked and removed sequencing
563 and optical duplicates, and realigned around indels in each mapped BAM file using Picard Version 2.23.4
564 and GATK Version 4.0.0.0 (HTTP://BROADINSTITUTE.GITHUB.IO/PICARD ; MCKENNA *et al.* 2010;
565 DEPRISTO *et al.* 2011). We then removed individuals with low coverage of the *D. innubila* genome (less
566 than 5x coverage for 80% of the non-repetitive genome), and individuals we suspected of being
567 misidentified as *D. innubila* following collection due to anomalous mapping. This left us with 280 *D.*
568 *innubila* wild flies (48 - 84 flies per populations) from 2017 and 38 wild flies from 2001 with at least 5x
569 coverage across at least 80% of the euchromatic genome (Supplementary Table 1).

570 *Nucleotide polymorphisms across the population samples*

571 For the 318 sequenced samples with reasonable coverage, we called SNPs using GATK HaplotypeCaller
572 Version bcf4.0.0.0 (MCKENNA *et al.* 2010; DEPRISTO *et al.* 2011) which generated a multiple strain VCF
573 file. We then used BCFtools Version 1.7 (NARASIMHAN *et al.* 2016) to remove sites with a GATK quality
574 score (a composite PHRED score for multiple samples per site) lower than 950 and sites absent (e.g. sites
575 of low quality, or with 0 coverage) from over 5% of individuals. This filtering left us with 4,522,699 SNPs
576 and small indels across the 168Mbp genome of *D. innubila*. We then removed SNPs found as a singleton
577 in a single population (as possible errors), leaving us with 3,240,198 SNPs. We used the annotation of *D.*
578 *innubila* and SNPeff Version 5.0 (CINGOLANI *et al.* 2012) to identify SNPs as synonymous, non-
579 synonymous, non-coding or another annotation. Simultaneous to the *D. innubila* population samples, we
580 also mapped genomic information from outgroup species *D. falleni* (SRA: SRR8651761) and *D. phalerata*
581 (SRA: SRR8651760) to the *D. innubila* genome and called divergence using the GATK variation calling
582 pipeline to identify derived polymorphisms and fixed differences in *D. innubila*.

583 *Population genetic summary statistics and structure*

584 Using the generated total VCF file with SNPeff annotations, we created a second VCF containing only
585 synonymous polymorphism using BCFtools Version 1.7 (NARASIMHAN *et al.* 2016). We calculated
586 pairwise diversity per base, Watterson's theta, Tajima's D (TAJIMA 1989) and F_{ST} (WEIR AND COCKERHAM
587 1984) (versus all other populations) across the genome for each gene in each population using VCFtools
588 Version 0.1.13 (DANECEK *et al.* 2011) and the VCF containing all variants. Using ANGSD Version 0.9.11
589 to parse the synonymous polymorphism VCF (KORNELIUSSEN *et al.* 2014), we generated synonymous
590 unfolded site frequency spectra for the *D. innubila* autosomes for each population, using the *D. falleni* and
591 *D. phalerata* genomes as outgroups to the *D. innubila* genome (HILL *et al.* 2019).

592 We used the population silent SFS with previously estimated mutation rates of *Drosophila*
593 (SCHRIDER et al. 2013), as inputs in StairwayPlot Version 2 (LIU AND FU 2015), to estimate the effective
594 population size backwards in time for each location.
595 We also estimated the extent of population structure across samples using Structure Version 2.3.4
596 (FALUSH *et al.* 2003), repeating the population assignment for each chromosome separately using only
597 silent polymorphism, for between one and ten populations (k = 1-10, 100000 iterations burn-in, 400000
598 iterations sampling). Following (FRICHOT *et al.* 2014), we manually assessed which number of
599 subpopulations best fits the data for each *D. innubila* chromosome and DiNV to minimize entropy.
600 As our populations have recently established, we used δaδi Version 1.6.7 to determine which
601 model of population dynamics best fits for each *D. innubila* chromosome (GUTENKUNST *et al.* 2010).For
602 pairs of populations, we compared models to determine if populations are behaving as one population
603 having gone through a bottleneck (*bottlegrowth* model), as split populations with migration
604 (*bottlegrowth_split_mig* model) or recently split populations with no migration (*bottlegrowth_split* model).
605 We generated a site frequency spectrum for each chromosome for each population from our VCF of silent
606 polymorphism in δaδi (though using the total polymorphism for the mitochondria), using the
607 *Spectrum.from_data_dict* function. For each pair of populations and each chromosome, we estimated the
608 optimal parameters for each model using the *Inference.optimize_log* function. We then fit each model
609 (using the *Inference.ll_multinom* function) and compared the fit of each model using a likelihood-ratio test,
610 to determine what demographic model best fits each Muller element and the mitochondria.

611 *Signatures of local adaptive divergence across D. innubila populations*
612 We downloaded gene ontology groups from Flybase (GRAMATES *et al.* 2017). We then used a gene
613 enrichment analysis to identify enrichments for particular gene categories among genes in the upper and
614 lower 2.5th percentile for F_{ST}, Tajima's D and Pairwise Diversity versus all other genes (SUBRAMANIAN *et*
615 *al.* 2005). Due to differences on the chromosomes Muller A and B versus other chromosomes in some
616 cases, we also repeated this analysis chromosome by chromosome, taking the upper 97.5th percentile of
617 each chromosome.
618 We next attempted to look for selective sweeps in each population using Sweepfinder2 (HUBER *et*
619 *al.* 2016). We reformatted the polarized VCF file to a folded allele frequency file, showing allele counts for
620 each base. We then used Sweepfinder2 Version 1.0 on the total called polymorphism in each population to
621 detect selective sweeps in 1kbp windows (HUBER *et al.* 2016). We reformatted the results and looked for
622 genes neighboring or overlapping with regions where selective sweeps have occurred with a high
623 confidence, shown as peaks above the genomic background. We surveyed for peaks by identifying 1kbp
624 windows in the 97.5th percentile and 99th percentile for composite likelihood ratio per chromosome.

625 Using the total VCF with outgroup information, we next calculated D_{XY} per SNP for all pairwise
626 population comparisons (NEI AND MILLER 1990), as well as within population pairwise diversity and d_S
627 from the outgroups, using a custom python script. We then found the average D_{XY} and d_S per gene and
628 looked for gene enrichments in the upper 97.5th percentile, versus all other genes.

629 *Inversions*

630 For each sample, we used Delly Version 2.0 (RAUSCH *et al.* 2012) to generate a multiple sample VCF file
631 identifying regions in the genome which are potentially duplicated, deleted or inverted compared to the
632 reference genome. Then we filtered and removed inversions found in fewer than 1% of individuals and with
633 a GATK VCF quality score lower than 200. We also called inversions using Pindel Version 0.2.5 (YE *et*
634 *al.* 2009) in these same samples and again removed low quality inversion calls. We next manually filtered
635 samples and merged inversions with breakpoints within 1000bp at both ends and significantly overlapping
636 in the presence/absence of these inversions across strains (using a χ^2 test, p-value < 0.05). We also filtered
637 and removed large inversions which were only found with one of the two tools. Using the remaining filtered
638 and merged inversions we estimated the frequency of each inversion within the total population.

639 *Signatures of recurrent selection*

640 We filtered the total VCF with annotations by SNPeff and retained only non-synonymous (replacement) or
641 synonymous (silent) SNPs (CINGOLANI *et al.* 2012). We then compared these polymorphisms to the
642 differences identified to *D. falleni* and *D. phalerata* to polarize changes to specific branches. Specifically,
643 we sought to determine sites which are polymorphic in our *D. innubila* populations or are substitutions
644 which fixed along the *D. innubila* branch of the phylogeny. We used the counts of fixed and polymorphic
645 silent and replacement sites per gene to estimate McDonald-Kreitman-based statistics, specifically direction
646 of selection (DoS) (MCDONALD AND KREITMAN 1991b; SMITH AND EYRE-WALKER 2002; STOLETZKI AND
647 EYRE-WALKER 2011). We also used these values in SnIPRE (EILERTSON *et al.* 2012), which reframes
648 McDonald-Kreitman based statistics as a linear model, taking into account the total number of non-
649 synonymous and synonymous mutations occurring in user defined categories to predict the expected
650 number of these substitutions and calculate a selection effect relative to the observed and expected number
651 of mutations (EILERTSON *et al.* 2012). We calculated the SnIPRE selection effect for each gene using the
652 total number of mutations on the chromosome of the focal gene. Using FlyBase gene ontologies
653 (GRAMATES *et al.* 2017), we sorted each gene into a category of immune gene or classed it as a background
654 gene, allowing a gene to be classed in multiple immune categories. We fit a GLM to identify functional
655 categories with excessively high estimates of adaptation, considering multiple covariates:

656 $$Statistic \sim Population + Gene\ group + (Gene\ group * Population) + Chromosome$$
657 $$+ Chromosome{:}Position$$

658 We then calculated the difference in each statistic between our focal immune genes and a randomly sampled
659 nearby (within 100kbp) background gene, finding the average of these differences for each immune
660 category over 10000 replicates, based on (CHAPMAN *et al.* 2019).

661 To confirm these results, we also used AsymptoticMK (HALLER AND MESSER 2017) to calculate
662 asymptotic α for each gene category. We generated the non-synonymous and synonymous site frequency
663 spectrum for each gene category, which we then used in AsymptoticMK to calculate asymptotic α and a
664 95% confidence interval. We then used a permutation test to assess if functional categories of interest
665 showed a significant difference in asymptotic α from the rest of categories.

666 **Acknowledgements**

667 This work was completed with helpful discussion from Justin Blumensteil, Joanne Chapman, Richard Glor,
668 Stuart MacDonald, Maria Orive and Caroyln Wessinger. We would especially like to thank Kelly Dyer and
669 Paul Guinsberg for proposing the idea of the manuscript and providing feedback on early sections of the
670 manuscript. We greatly appreciate help provided by John Kelly, for providing scripts to calculate D_{XY} as
671 well as advice on population genetic inference and comments on the manuscript. Collections were
672 completed with assistance from Todd Schlenke and the Southwest Research Station. We thank Brittny Smith
673 and the KU CMADP Genome Sequencing Core (NIH Grant P20 GM103638) for assistance in genome
674 isolation, library preparation and sequencing. This work was supported by a K-INBRE postdoctoral grant
675 to TH (NIH Grant P20 GM103418). This work was also funded by NIH Grants R00 GM114714 and R01
676 AI139154 to RLU.

677 **Data Availability**

678 All sequencing information is available on the NCBI SRA (SRA: SRP187240), while all genomes used in
679 this study are available on the NCBI genome database (SRA: GCA_004354385.1, GCA_005876895.1).
680 All supplementary data used in this manuscript is available at:
681 https://figshare.com/projects/innubila_population_genomics/87662

682

683 **Bibliography**

684 Antunes, J. T., P. N. Leao and V. M. Vasconcelos, 2015 *Cylindrospermopsis raciborskii:* review
685 of the distribution, phylogeography, and ecophysiology of a global invasive species.
686 Frontiers in Microbiology 6**:** 473.
687 Arechederra-Romero, L., 2012 Southwest Fire Science Consortium Field Trip to the Chiricahua
688 National Monument: Discussion of the Impacts of the 2011 Horseshoe 2 Fire, pp. in
689 *Arizona Geology Magazine*, Arizona Geology Magazine.
690 Arizona-Geological-Survey, 2005 Arizona Geology. Arizona Geology 35**:** 1-6.
691 Astanei, I., E. Gosling, J. Wilson and E. Powell, 2005 Genetic variability and phylogeography of
692 the invasive zebra mussel, *Dreissena polymorpha (Pallas)*. Mol Ecol 14**:** 1655-1666.
693 Avgar, T., G. Street, and J. M. Fryxell, 2014 On the adaptive benefits of mammal migration.
694 Canadian Journal of Zoology 92**:** 481-490.
695 Behrman, E. L., S. S. Watson, K. R. O'Brien, S. M. Heschel and P. S. Schmidt, 2015 Seasonal
696 variation in life history traits in two *Drosophila* species. Journal of Evolutionary Biology
697 28**:** 1691-1704.
698 Buffalo, V., 2018 *Scythe*.
699 Cai, J. J., J. M. Macpherson, G. Sella and D. a. Petrov, 2009 Pervasive hitchhiking at coding and
700 regulatory sites in humans. PLoS genetics 5**:** 1-13.
701 Chakraborty, M., R. Zhao, X. Zhang, S. Kalsow and J. J. Emerson, 2017 Extensive hidden genetic
702 variation shapes the structure of functional elements in *Drosophila*. Doi.Org 50**:** 114967.
703 Chapman, J. R., T. Hill and R. L. Unckless, 2019 Balancing selection drives maintenance of
704 genetic variation in *Drosophila* antimicrobial peptides. Genome Biology and Evolution 11**:**
705 2691-2701.
706 Charlesworth, B., D. Charlesworth and N. H. Barton, 2003 The Effects of Genetic and Geographic
707 Structure on Neutral Variation. Annual Review of Ecology, Evolution, and Systematics
708 34**:** 99-125.
709 Charlesworth, B., M. T. Morgan and D. Charlesworth, 1993 The effect of deleterious mutations
710 on neutral molecular variation. Genetics 134**:** 1289-1303.
711 Chen, X., O. Schulz-Trieglaff, R. Shaw, B. Barnes, F. Schlesinger *et al.*, 2016 Manta: Rapid
712 detection of structural variants and indels for germline and cancer sequencing applications.
713 Bioinformatics 32**:** 1220-1222.
714 Cingolani, P., A. Platts, L. L. Wang, M. Coon, T. Nguyen *et al.*, 2012 A program for annotating
715 and predicting the effects of single nucleotide polymorphisms, SnpEff: SNPs in the genome
716 of *Drosophila melanogaster* strain w1118; iso-2; iso-3. Fly 6**:** 80-92.
717 Cini, A., C. Ioriatti and G. Anfora, 2012 A review of the invasion of *Drosophila suzukii* in Europe
718 and a draft research agenda for integrated pest management. Bulletin of Insectology 65**:**
719 149-160.
720 Cloudsley-Thompson, J. L., 1978 Human Activities and Desert Expansion. The Geographical
721 Journal 144**:** 416-423.
722 Coe, S. J., D. M. Finch and M. M. Friggens, 2012 An Assessment of Climate Change and the
723 Vulnerability of Wildlife in the Sky Islands of the Southwest, pp. 1-208. United States
724 Department of Agriculture.
725 Crimmins, T. M., M. A. Crimmins and C. D. Bertelsen, 2011 Onset of summer flowering in a 'Sky
726 Island' is driven by monsoon moisture. New Phytol 191**:** 468-479.

Cruickshank, T. E., and M. W. Hahn, 2014 Reanalysis suggests that genomic islands of speciation are due to reduced diversity, not reduced gene flow. Mol Ecol 23**:** 3133-3157.

Cutter, A. D., and B. A. Payseur, 2013 Genomic signatures of selection at linked sites: unifying the disparity among species. Nat Rev Genet 14**:** 262-274.

Danecek, P., A. Auton, G. Abecasis, C. A. Albers, E. Banks *et al.*, 2011 The variant call format and VCFtools. Bioinformatics 27**:** 2156-2158.

DePristo, M. A., E. Banks, R. Poplin, K. V. Garimella, J. R. Maguire *et al.*, 2011 A framework for variation discovery and genotyping using next-generation DNA sequencing data. Nature genetics 43**:** 491-498.

Dobzhansky, T., and B. Spassky, 1968 The Genetics of Natural Populations XL: Heterotic and Deleterious Effects of Recessive Lethals in Populations of *Drosophila pseudoobscura*. Genetics 59**:** 411-425.

Dobzhansky, T., and A. H. Sturtevant, 1937 Inversions In Chromosomes of *Drosophila pseudoobscura.* Genetics 23**:** 28-64.

Dobzhansky, T. H., A. S. Hunter, O. Pavlovsky, B. Spassky and B. Wallace, 1963 Genetics of natural populations. XXXI. Genetics of an isolated marginal population of *Drosophila pseudoobscura*. Genetics 48**:** 91-103.

Dostert, C., E. Jouanguy, P. Irving, L. Troxler, D. Galiana-Arnoux *et al.*, 2005 The Jak-STAT signaling pathway is required but not sufficient for the antiviral response of *Drosophila.* Nat Immunol 6**:** 946-953.

Dyer, K. A., 2004 Evolutionarily Stable Infection by a Male-Killing Endosymbiont in *Drosophila innubila*: Molecular Evidence From the Host and Parasite Genomes. Genetics 168**:** 1443-1455.

Dyer, K. a., and J. Jaenike, 2005 Evolutionary dynamics of a spatially structured host-parasite association: Drosophila innubila and male-killing Wolbachia. Evolution; international journal of organic evolution 59**:** 1518-1528.

Dyer, K. A., M. S. Minhas and J. Jaenike, 2005 Expression and modulation of embryonic male-killing in *Drosophila innubila*: opportunities for multilevel selection. Evolution; international journal of organic evolution 59**:** 838-848.

Eilertson, K. E., J. G. Booth and C. D. Bustamante, 2012 SnIPRE: Selection Inference Using a Poisson Random Effects Model. PLoS Computational Biology 8.

Excoffier, L., M. Foll and R. J. Petit, 2009 Genetic Consequences of Range Expansions. Annual Review of Ecology, Evolution, and Systematics 40**:** 481-501.

Falush, D., M. Stephens and J. K. Pritchard, 2003 Inference of population structure using multilocus genotype data: Linked loci and correlated allele frequencies. Genetics 164**:** 1567-1587.

Fave, M. J., R. A. Johnson, S. Cover, S. Handschuh, B. D. Metscher *et al.*, 2015 Past climate change on Sky Islands drives novelty in a core developmental gene network and its phenotype. BMC Evol Biol 15**:** 183.

Frichot, E., F. Mathieu, T. Trouillon, G. Bouchard and O. François, 2014 Fast and efficient estimation of individual ancestry coefficients. Genetics 196**:** 973-983.

Fuller, Z. L., G. D. Haynes, S. Richards and S. W. Schaeffer, 2016 Genomics of Natural Populations: How Differentially Expressed Genes Shape the Evolution of Chromosomal Inversions in. Genetics.

Gao, Z., D. Waggoner, M. Stephens, C. Ober and M. Przeworski, 2015 An estimate of the average number of recessive lethal mutations carried by humans. Genetics 199**:** 1243-1254.

773 Gillespie, J., 2004 Population Genetics: A Concise Guide. 232.
774 Gramates, L. S., S. J. Marygold, G. Dos Santos, J. M. Urbano, G. Antonazzo *et al.*, 2017 FlyBase
775 at 25: Looking to the future. Nucleic Acids Research 45**:** D663-D671.
776 Guindon, S., J.-F. Dufayard, V. Lefort, M. Anisimova, W. Hordijk *et al.*, 2010 New algorithms
777 and methods to estimate maximum-likelihood phylogenies: assessing the performance of
778 PhyML 3.0. Systematic biology 59**:** 307-321.
779 Gutenkunst, R. N., R. D. Hernandez, S. H. Williamson and C. D. Bustamante, 2010 Diffusion
780 Approximations for Demographic Inference: ∂a∂i. Nature precedings.
781 Haller, B. C., and P. W. Messer, 2017 asymptoticMK: A Web-Based Tool for the Asymptotic
782 McDonald–Kreitman Test. G3: Genes, Genomes, Genetics 7**:** 1569-1575.
783 Hermisson, J., and P. S. Pennings, 2005 Soft sweeps: molecular population genetics of adaptation
784 from standing genetic variation. Genetics 169**:** 2335-2352.
785 Hewitt, G., 2000 The genetic legacy of the Quaternary ice ages. Nature 405**:** 907-913.
786 Hill, T., B. Koseva and R. L. Unckless, 2019 The genome of *Drosophila innubila* reveals lineage-
787 specific patterns of selection in immune genes. Molecular Biology and Evolution**:** 1-36.
788 Hill, T., and R. Unckless, 2020 Recurrent evolution of two competing haplotypes in an insect DNA
789 virus. Biorxiv**:** 1-45.
790 Hoban, S., J. L. Kelley, K. E. Lotterhos, M. F. Antolin, G. Bradburd *et al.*, 2016 Finding the
791 Genomic Basis of Local Adaptation: Pitfalls, Practical Solutions, and Future Directions.
792 Am Nat 188**:** 379-397.
793 Hoffmann, J. A., 2003 The immune response of *Drosophila*. Nature 426**:** 33-38.
794 Holmgren, K., J. A. Lee-Thorp, G. R. J. Cooper, K. Lundblad, T. C. Partridge *et al.*, 2003 Persistent
795 millennial-scale climatic variability over the past 25,000 years in Southern Africa.
796 Quaternary Science Reviews 22**:** 2311-2326.
797 Http://broadinstitute.github.io/picard, *Picard*.
798 Huber, C. D., M. DeGiorgio, I. Hellmann and R. Nielsen, 2016 Detecting recent selective sweeps
799 while controlling for mutation rate and background selection. Mol Ecol 25**:** 142-156.
800 Imler, J., and I. Elftherianos, 2009 *Drosophila* as a model for studying antiviral defences. Insect
801 infection and immunity (eds Rolff J., Reyolds SE)**:** 49-68.
802 Jaenike, J., and K. A. Dyer, 2008 No resistance to male-killing *Wolbachia* after thousands of years
803 of infection. Journal of Evolutionary Biology 21**:** 1570-1577.
804 Jaenike, J., K. A. Dyer and L. K. Reed, 2003 Within-population structure of competition and the
805 dynamics of male-killing *Wolbachia*. Evolutionary Ecology Research 5**:** 1023-1036.
806 Jaenike, J., and S. J. Perlman, 2002 Ecology and Evolution of Host-Parasite Associations:
807 Mycophagous *Drosophila* and Their Parasitic Nematodes. The American Naturalist 160**:**
808 S23-S39.
809 Joshi, N., and J. Fass, 2011 Sickle: A sliding window, adaptive, quality-based trimming tool for
810 fastQ files. 1.33.
811 Kapun, M., D. K. Fabian, J. Goudet and T. Flatt, 2016 Genomic Evidence for Adaptive Inversion
812 Clines in Drosophila melanogaster. Mol Biol Evol 33**:** 1317-1336.
813 Kimbrell, D. A., and B. Beutler, 2001 The evolution and genetics of innate immunity. Nat Rev
814 Genet 2**:** 256-267.
815 Korneliussen, T. S., A. Albrechtsen and R. Nielsen, 2014 ANGSD: Analysis of Next Generation
816 Sequencing Data. BMC Bioinformatics 15**:** 356.
817 Lack, J. B., C. M. Cardeno, M. W. Crepeau, W. Taylor, R. B. Corbett-Detig *et al.*, 2015 The
818 *Drosophila* genome nexus: A population genomic resource of 623 *Drosophila*

melanogaster genomes, including 197 from a single ancestral range population. Genetics 199: 1229-1241.

Li, H., and R. Durbin, 2009 Fast and accurate short read alignment with Burrows-Wheeler transform. Bioinformatics (Oxford, England) 25: 1754-1760.

Li, H., and R. Durbin, 2011 Inference of human population history from individual whole-genome sequences. Nature 475: 493-496.

Li, H., B. Handsaker, A. Wysoker, T. Fennell, J. Ruan *et al.*, 2009 The sequence alignment/map format and SAMtools. Bioinformatics (Oxford, England) 25: 2078-2079.

Liu, X., and Y.-X. Fu, 2015 Exploring population size changes using SNP frequency spectra. Nature genetics 47: 555-559.

Ma, X., J. L. Kelley, K. Eilertson, S. Musharoff, J. D. Degenhardt *et al.*, 2013 Population Genomic Analysis Reveals a Rich Speciation and Demographic History of Orangutans (*Pongo pygmaeus* and *Pongo abelii*). PLoS ONE 8.

Machado, C. a., T. S. Haselkorn and M. a. F. Noor, 2007 Evaluation of the genomic extent of effects of fixed inversion differences on intraspecific variation and interspecific gene flow in *Drosophila pseudoobscura* and *Drosophila persimilis*. Genetics 175: 1289-1306.

Machado, H. E., A. O. Bergland, K. R. O'Brien, E. L. Behrman, P. S. Schmidt *et al.*, 2015 Comparative population genomics of latitudinal variation in *D. simulans* and *D. melanogaster*. Molecular Ecology: n/a-n/a.

Mackay, T. F. C., S. Richards, E. a. Stone, A. Barbadilla, J. F. Ayroles *et al.*, 2012 The *Drosophila melanogaster* genetic reference panel. Nature 482: 173-178.

Manthey, J. D., and R. G. Moyle, 2015 Isolation by environment in White-breasted Nuthatches (Sitta carolinensis) of the Madrean Archipelago sky islands: a landscape genomics approach. Mol Ecol 24: 3628-3638.

Marinkovic, D., 1967 Genetic Loads Affecting Fecundity in Natural Populations of *Drosophila pseudoobscura*. Genetics: 61-71.

Markow, T. A., and P. O'Grady, 2006 *Drosophila*: a guide to species identification.

Martin, M., 2011 Cutadapt removes adapter sequences from high-throughput sequencing reads. Technical Notes: 1-12.

Marzo, M., M. Puig and A. Ruiz, 2008 The Foldback-like element Galileo belongs to the P superfamily of DNA transposons and is widespread within the Drosophila genus. Proceedings of the National Academy of Sciences of the United States of America 105: 2957-2962.

Matthey-Doret, R., and M. C. Whitlock, 2018 Background selection and the statistics of population differentiation: consequences for detecting local adaptation. Biorxiv: 1-5.

McCormack, J. E., H. Huang and L. L. Knowles, 2009 Sky Islands, pp. 841-843 in *Encyclopedia of islands*.

McDonald, J. H., and M. Kreitman, 1991a Adaptive protein evolution at the Adh locus in *Drosophila*. Nature 351: 652-654.

McDonald, J. H., and M. Kreitman, 1991b Adaptive protein evolution at the Adh locus in *Drosophila*. Nature 351: 652-654.

McKenna, A., M. Hanna, E. Banks, A. Sivachenko, K. Cibulskis *et al.*, 2010 The Genome Analysis Toolkit: A MapReduce framework for analyzing next-generation DNA sequencing data. Proceedings of the International Conference on Intellectual Capital, Knowledge Management & Organizational Learning 20: 1297-1303.

McVean, G., 2007 The structure of linkage disequilibrium around a selective sweep. Genetics 175: 1395-1406.

Merkling, S. H., and R. P. van Rij, 2013 Beyond RNAi: Antiviral defense strategies in *Drosophila* and mosquito. Journal of Insect Physiology 59: 159-170.

Messer, P. W., and D. A. Petrov, 2012 The McDonald-Kreitman Test and its Extensions under Frequent Adaptation: Problems and Solutions. Proceedings of the National Academy of Sciences 110: 8615-8620.

Messer, P. W., and D. A. Petrov, 2013 Population genomics of rapid adaptation by soft selective sweeps. Trends in Ecology & Evolution 28: 659-669.

Misztal, L. W., G. Garfin and L. Hansen, 2013 Responding to Climate Change Impacts in the Sky Island Region: From Planning to Action. USDA Forest Service Proceedings P67.

Narasimhan, V., P. Danecek, A. Scally, Y. Xue, C. Tyler-Smith *et al.*, 2016 BCFtools/RoH: A hidden Markov model approach for detecting autozygosity from next-generation sequencing data. Bioinformatics 32: 1749-1751.

Nei, M., 1987 *Molecular evolutionary genetics*. Columbia university press.

Nei, M., and J. Miller, 1990 A Simple Method for Estimating Average Number of Nucleotide Substitutions Within and Between Populations From Restriction Data. Genetics 125: 873-879.

Nielsen, R., 2005 Molecular signatures of natural selection. Annu Rev Genet 39: 197-218.

Noor, M. a. F., D. a. Garfield, S. W. Schaeffer and C. a. Machado, 2007 Divergence between the *Drosophila pseudoobscura* and *D. persimilis* genome sequences in relation to chromosomal inversions. Genetics 177: 1417-1428.

Oneal, E., D. B. Lowry, K. M. Wright, Z. Zhu and J. H. Willis, 2014 Divergent population structure and climate associations of a chromosomal inversion polymorphism across the Mimulus guttatus species complex. Mol Ecol 23: 2844-2860.

Palmer, W. H., J. Joosten, G. J. Overheul, P. W. Jansen, M. Vermeulen *et al.*, 2018 Induction and suppression of NF- κB signalling by a DNA virus of *Drosophila.*

Parmesan, C., and G. Yohe, 2003 A globally coherent fingerprint of climate change impacts across natural systems. Nature 421: 37-42.

Patterson, J. T., 1954 Studies in the genetics of *Drosophila.*, pp.

Patterson, J. T., and W. S. Stone, 1949 Studies in the genetics of *Drosophila*., pp. 7-17 in *University of Texas Publications*.

Perlman, S. J., G. S. Spicer, D. Dewayne Shoemaker and J. Jaenike, 2003 Associations between mycophagous *Drosophila* and their *Howardula* nematode parasites: A worldwide phylogenetic shuffle. Molecular Ecology 12: 237-249.

Pool, J., and C. H. Langley, 2013 DPGP3.

Pool, J. E., R. B. Corbett-detig, R. P. Sugino, K. A. Stevens, C. M. Cardeno *et al.*, 2012 Population Genomics of Sub-Saharan *Drosophila melanogaster:* African Diversity and Non-African Admixture. PLoS Genetics 8: 1-24.

Porretta, D., V. Mastrantonio, R. Bellini, P. Somboon and S. Urbanelli, 2012 Glacial history of a modern invader: phylogeography and species distribution modelling of the Asian tiger mosquito Aedes albopictus. PLoS One 7: e44515.

Przeworski, M., G. Coop, J. D. Wall and S. Url, 2011 The Signature of Positive Selection on Standing Genetic Variation. Evolution 59: 2312-2323.

Puzey, J. R., J. H. Willis and J. K. Kelly, 2017 Population structure and local selection yield high genomic variation in Mimulus guttatus. Mol Ecol 26: 519-535.

910 Rankin, M. A., and J. C. A. Burchsted, 1992 The Cost of Migration in Insects. Annual Review of
911 Entymology 37: 533-559.
912 Rastogi, S., and D. a. Liberles, 2005 Subfunctionalization of duplicated genes as a transition state
913 to neofunctionalization. BMC evolutionary biology 5: 28.
914 Rausch, T., T. Zichner, A. Schlattl, A. M. Stutz, V. Benes *et al.*, 2012 DELLY: structural variant
915 discovery by integrated paired-end and split-read analysis. Bioinformatics 28: i333-i339.
916 Rodriguez-Trelles, F., G. Alvarez and C. Zapata, 1996 Time-Series Analysis of Seasonal Changes
917 of the 0 Inversion polymorphism of Drosqphiila subobscura. Genetics 142: 179-187.
918 Rosenzweig, C., D. Karoly, M. Vicarelli, P. Neofotis, Q. Wu *et al.*, 2008 Attributing physical and
919 biological impacts to anthropogenic climate change. Nature 453: 353-357.
920 Schrider, D. R., D. Houle, M. Lynch and M. W. Hahn, 2013 Rates and genomic consequences of
921 spontaneous mutational events in Drosophila melanogaster. Genetics 194: 937-954.
922 Scott Chialvo, C. H., and T. Werner, 2018 Drosophila, destroying angels, and deathcaps! Oh my!
923 A review of mycotoxin tolerance in the genus Drosophila. Frontiers in Biology 13: 91-102.
924 Searle, J. B., P. Kotlik, R. V. Rambau, S. Markova, J. S. Herman *et al.*, 2009 The Celtic fringe of
925 Britain: insights from small mammal phylogeography. Proc Biol Sci 276: 4287-4294.
926 Sella, G., D. A. Petrov, M. Przeworski and P. Andolfatto, 2009 Pervasive natural selection in the
927 Drosophila genome? PLoS Genet 5: e1000495.
928 Shoemaker, D. D., V. Katju and J. Jaenike, 1999 *Wolbachia* and the evolution of reproductive
929 isolation between *Drosophila recens* and *Drosophila subquinaria*. Evolution 53: 1157-
930 1164.
931 Smit, A. F. A., and R. Hubley, 2013-2015 RepeatMasker Open-4.0, pp. RepeatMasker.
932 Smith, C. I., and B. D. Farrell, 2005 Phylogeography of the longhorn cactus beetle Moneilema
933 appressum LeConte (Coleoptera: Cerambycidae): was the differentiation of the Madrean
934 sky islands driven by Pleistocene climate changes? Mol Ecol 14: 3049-3065.
935 Smith, F. A., J. L. Betancourt and J. H. Brown, 1995 Evolution of Body Size in the Woodrat Over
936 the Past 25,000 Years of Climate Change. Science 270: 2012-2014.
937 Smith, N. G. C., and A. Eyre-Walker, 2002 Adaptive protein evolution in *Drosophila*. Nature 415:
938 1022-1024.
939 Stajich, J. E., and M. W. Hahn, 2005 Disentangling the effects of demography and selection in
940 human history. Mol Biol Evol 22: 63-73.
941 Stoletzki, N., and A. Eyre-Walker, 2011 Estimation of the neutrality index. Molecular Biology and
942 Evolution 28: 63-70.
943 Subramanian, A., P. Tamayo, V. K. Mootha, S. Mukherjee, B. L. Ebert *et al.*, 2005 Gene set
944 enrichment analysis: A knowledge-based approach for interpreting genome-wide
945 expression profiles. PNAS 102: 15545–15550.
946 Tajima, F., 1989 Statistical method for testing the neutral mutation hypothesis by DNA
947 polymorphism. Genetics 123: 585-595.
948 Takeda, K., and S. Akira, 2005 Toll-like receptors in innate immunity. International Immunology
949 17: 1-14.
950 Tigano, A., and V. L. Friesen, 2016 Genomics of local adaptation with gene flow. Mol Ecol 25:
951 2144-2164.
952 Unckless, R. L., 2011 A DNA Virus of *Drosophila*. PLoS ONE 6: e26564.
953 Unckless, R. L., and J. Jaenike, 2011 Maintenance of a Male-Killing *Wolbachia* in *Drosophila*
954 *innubila* By Male-Killing Dependent and Male-Killing Independent Mechanisms.
955 Evolution 66: 678-689.

Vicoso, B., and D. Bachtrog, 2015 Numerous Transitions of Sex Chromosomes in Diptera. PLoS Biology 13**:** 1-22.

Walsh, D. B., M. P. Bolda, R. E. Goodhue, A. J. Dreves, J. Lee *et al.*, 2011 *Drosophila suzukii* (Diptera: *Drosophilidae*): Invasive Pest of Ripening Soft Fruit Expanding its Geographic Range and Damage Potential. Journal of Integrated Pest Management 2**:** 1-7.

Watanabe, T. K., O. Yamaguchi and T. Mukai, 1974 The Genetic Variability of Third Chromosomes in a Local Population of *Drosophila melanogaster*. Genetics 82**:** 63-82.

Weir, B. S., and C. C. Cockerham, 1984 Estimating F-Statistics for the Analysis of Population Structure. Evolution 38**:** 1358-1370.

Werren, J. H., L. Baldo and M. E. Clark, 2008 Wolbachia: master manipulators of invertebrate biology. Nat Rev Microbiol 6**:** 741-751.

White, T. A., S. E. Perkins, G. Heckel and J. B. Searle, 2013 Adaptive evolution during an ongoing range expansion: the invasive bank vole (*Myodes glareolus*) in Ireland. Mol Ecol 22**:** 2971-2985.

Wiens, J. J., A. Camacho, A. Goldberg, T. Jezkova, M. E. Kaplan *et al.*, 2019 Climate change, extinction, and Sky Island biogeography in a montane lizard. Mol Ecol 28**:** 2610-2624.

Wright, S. I., B. Lauga and D. Charlesworth, 2003 Subdivision and haplotype structure in natural populations of *Arabidopsis lyrata*. Molecular Ecology 12**:** 1247–1263.

Ye, K., M. H. Schulz, Q. Long, R. Apweiler and Z. Ning, 2009 Pindel : a pattern growth approach to detect break points of large deletions and medium sized insertions from paired-end short reads. Bioinformatics 25**:** 2865-2871.

Zambon, R. A., M. Nandakumar, V. N. Vakharia and L. P. Wu, 2005 The Toll pathway is important for an antiviral response in *Drosophila*. Proceedings of the National Academy of Sciences 102**:** 7257-7262.

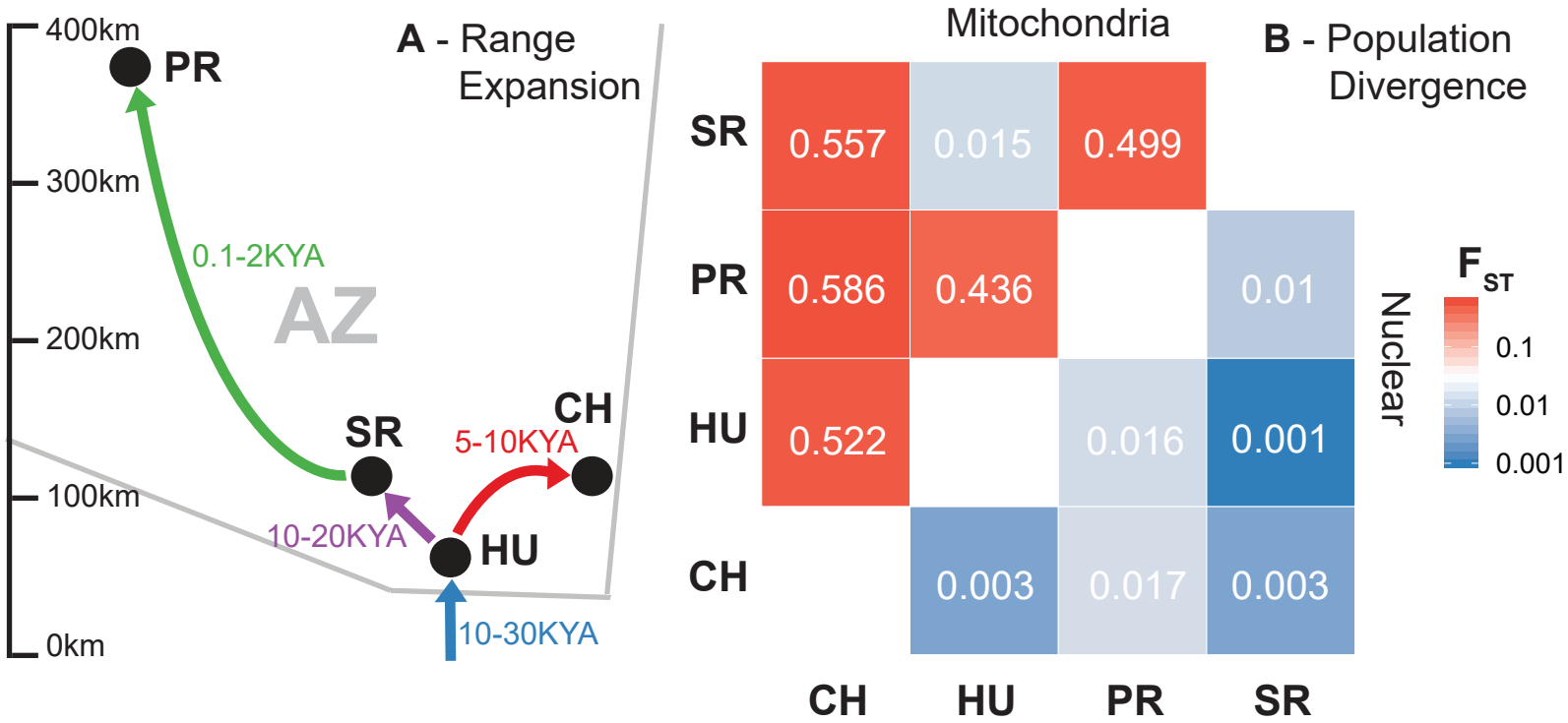
A - Range Expansion
400km
300km
200km
100km
0km
PR
SR
HU
CH
AZ
0.1-2KYA
5-10KYA
10-20KYA
10-30KYA
Mitochondria
B - Population Divergence
Nuclear
SR 0.557 0.015 0.499
PR 0.586 0.436 0.01
HU 0.522 0.016 0.001
CH 0.003 0.017 0.003
CH HU PR SR
F ST
0.1
0.01
0.001

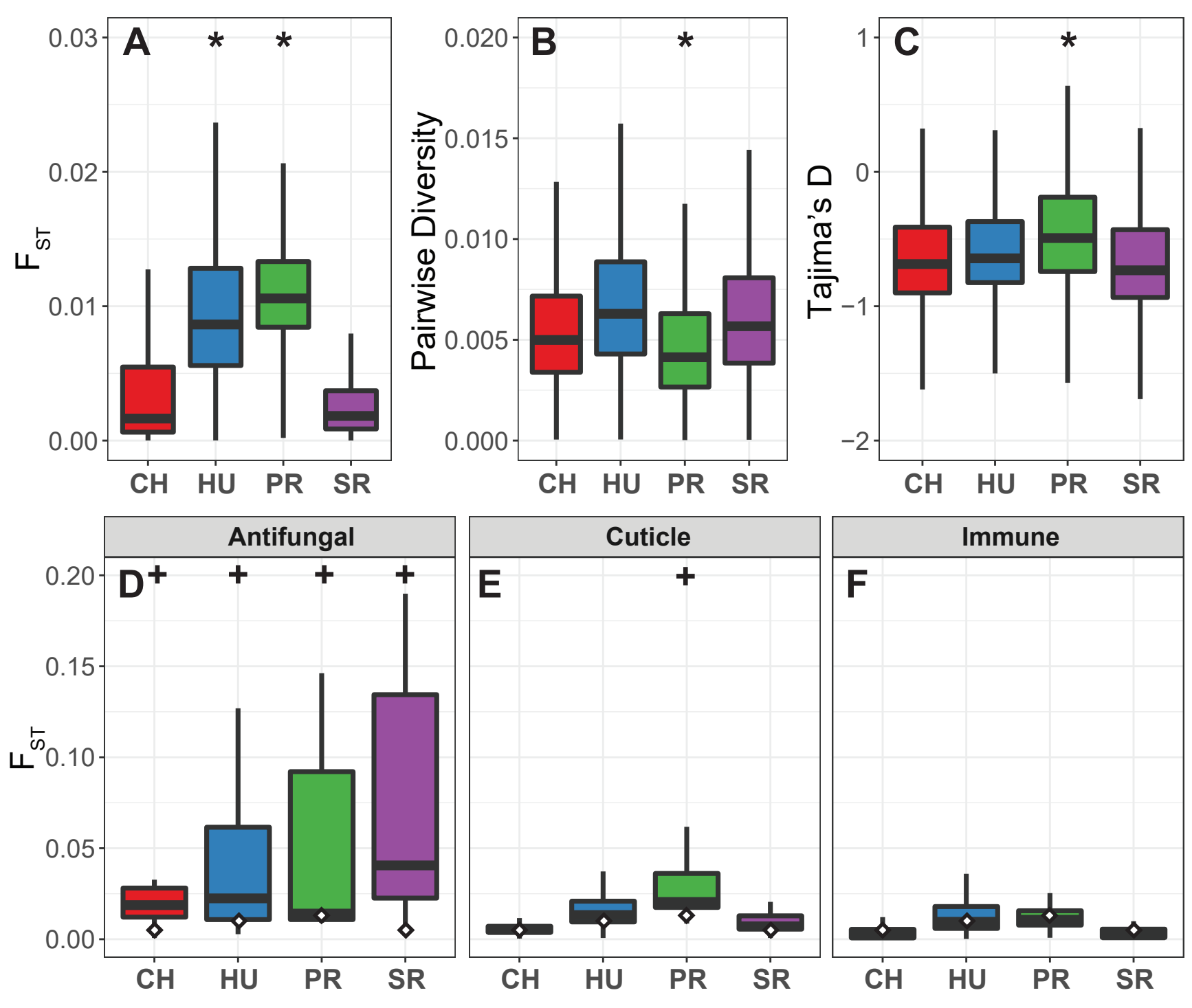
A
B
C
D
E
F
F_{ST}
Pairwise Diversity
Tajima's D
0.03
0.02
0.01
0.00
0.020
0.015
0.010
0.005
0.000
1
0
−1
−2
0.20
0.15
0.10
0.05
0.00
CH
HU
PR
SR
Antifungal
Cuticle
Immune

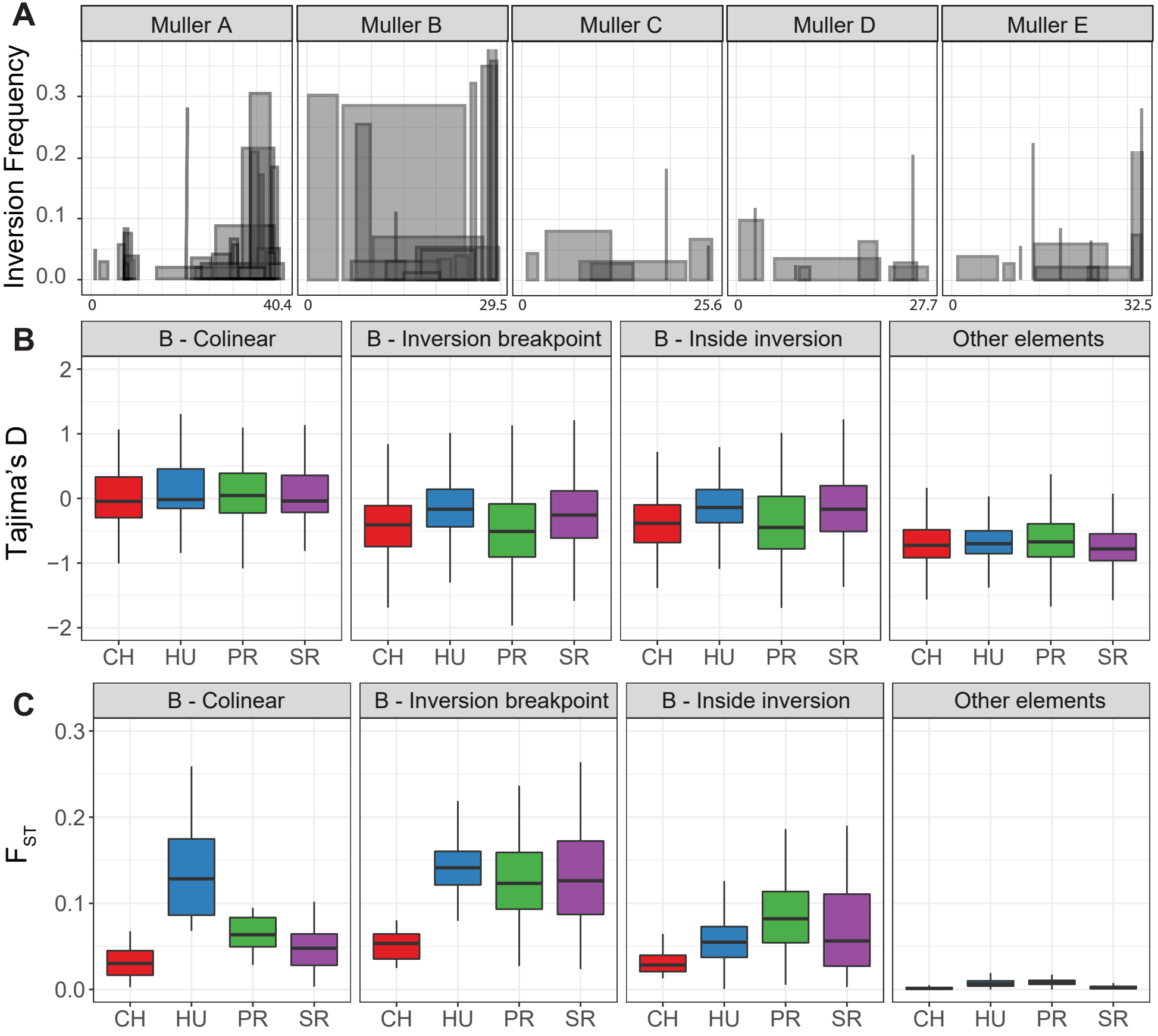
A
Muller A
Muller B
Muller C
Muller D
Muller E
Inversion Frequency
0.3
0.2
0.1
0.0
0
40.4
0
29.5
0
25.6
0
27.7
0
32.5
B
B - Colinear
B - Inversion breakpoint
B - Inside inversion
Other elements
Tajima's D
2
1
0
−1
−2
CH
HU
PR
SR
C
B - Colinear
B - Inversion breakpoint
B - Inside inversion
Other elements
F_{ST}
0.3
0.2
0.1
0.0
CH
HU
PR
SR

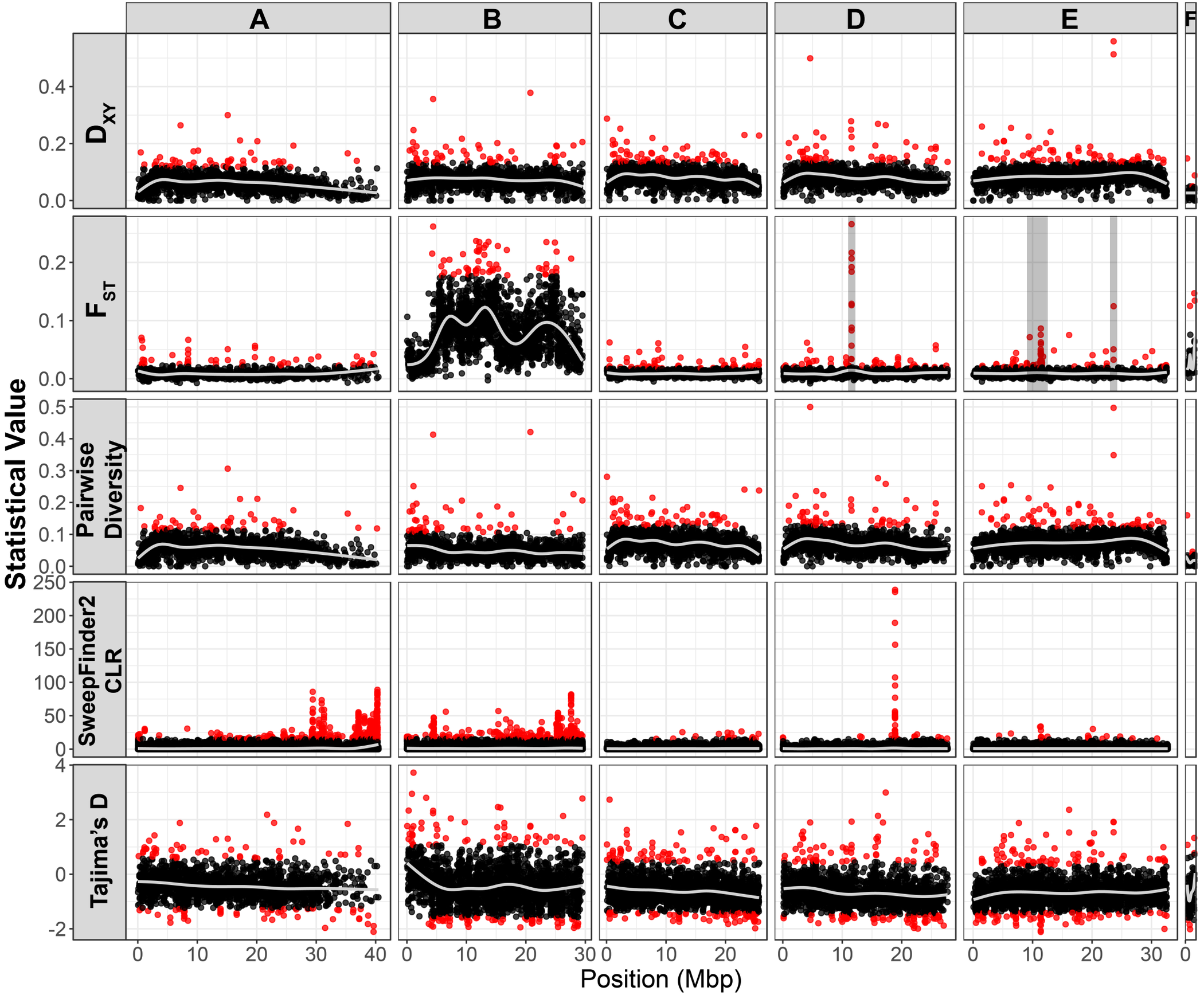
A
B
C
D
E
F
Statistical Value
D_{XY}
F_{ST}
Pairwise Diversity
SweepFinder2 CLR
Tajima's D
Position (Mbp)

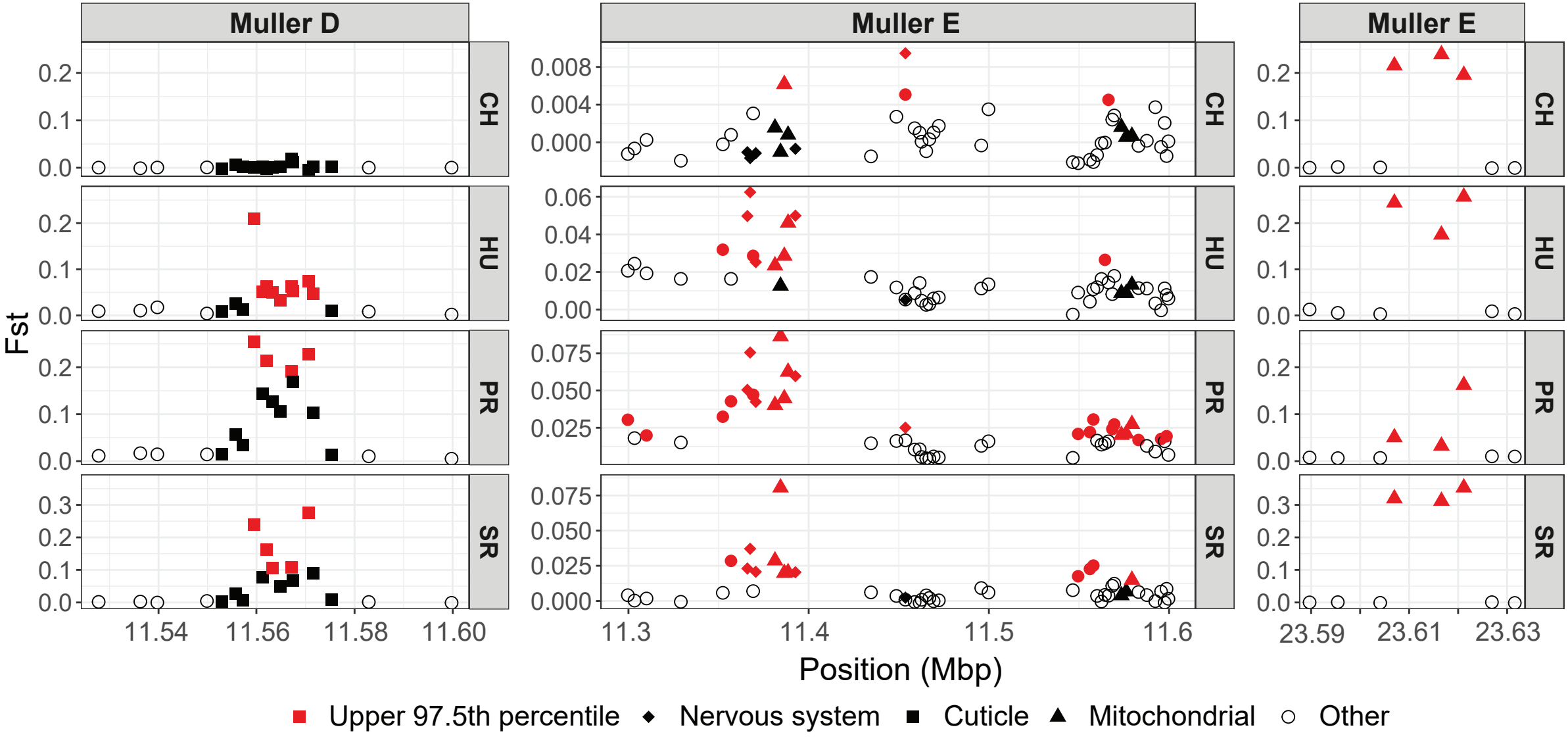
Muller D
Muller E
Muller E
CH
HU
PR
SR
Fst
0.0
0.1
0.2
0.3
0.000
0.004
0.008
0.02
0.04
0.06
0.025
0.050
0.075
11.54
11.56
11.58
11.60
11.3
11.4
11.5
11.6
23.59
23.61
23.63
Position (Mbp)
Upper 97.5th percentile
Nervous system
Cuticle
Mitochondrial
Other

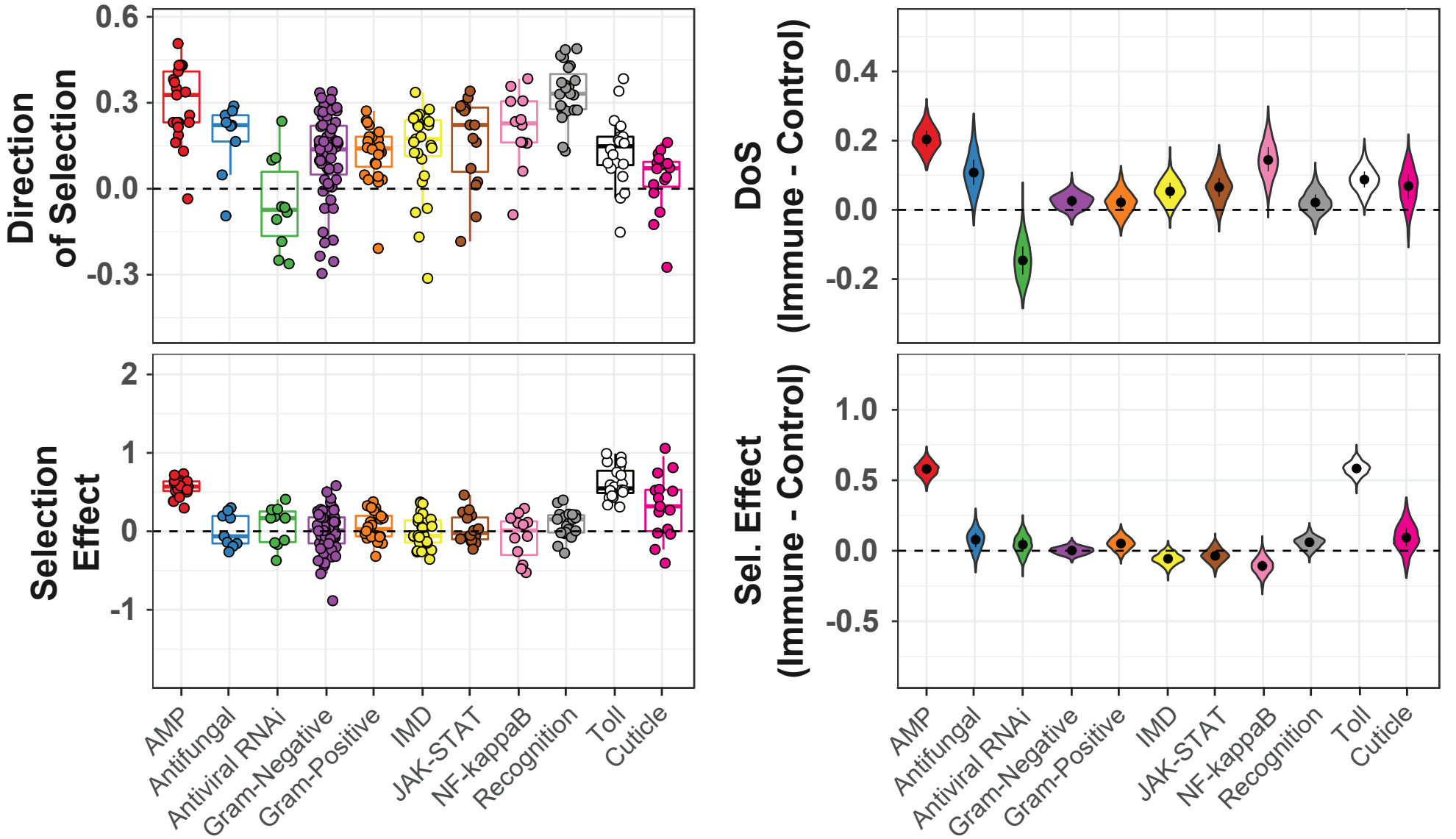
Direction of Selection
0.6
0.3
0.0
-0.3
DoS (Immune - Control)
0.4
0.2
0.0
-0.2
Selection Effect
2
1
0
-1
Sel. Effect (Immune - Control)
1.0
0.5
0.0
-0.5
AMP
Antifungal
Antiviral RNAi
Gram-Negative
Gram-Positive
IMD
JAK-STAT
NF-kappaB
Recognition
Toll
Cuticle

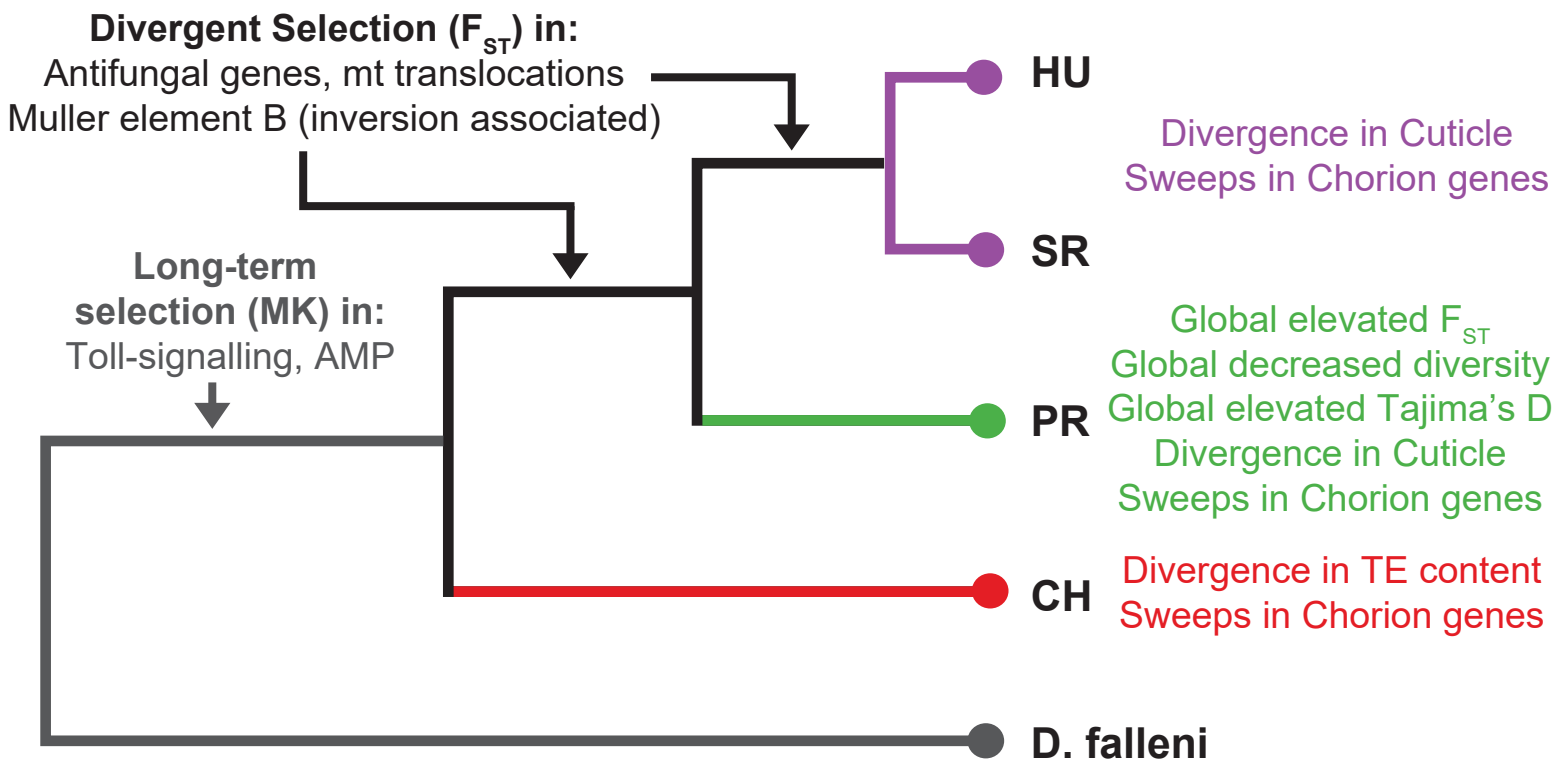
Divergent Selection (F_{ST}) in:
Antifungal genes, mt translocations
Muller element B (inversion associated)
Long-term selection (MK) in:
Toll-signalling, AMP
HU
SR
PR
CH
D. falleni
Divergence in Cuticle
Sweeps in Chorion genes
Global elevated F_{ST}
Global decreased diversity
Global elevated Tajima's D
Divergence in Cuticle
Sweeps in Chorion genes
Divergence in TE content
Sweeps in Chorion genes